1-17-2017

Automatic analysis of surface electromyography of reflexes for central nervous system inhibition during pregnancy

Neda Parvin
Rowan University

AUTOMATIC ANALYSIS OF SURFACE ELECTROMYOGRAPHY OF REFLEXES FOR CENTRAL NERVOUS SYSTEM INHIBITION DURING PREGNANCY

by

Neda Parvin

A Thesis

Submitted to the
Department of Electrical and Computer Engineering
College of Engineering
In partial fulfillment of the requirement
For the degree of
Master of Science in Electrical and Computer Engineering
at
Rowan University
November 9, 2016

Thesis Chair: Nidhal Bouaynaya, Ph.D.

Dedication

I would like to dedicate this work to my family who kept me all through the journey of completing this work and to Dr. Jamal Jon Derakhshan who dedicated his time on this research and helped me a lot.

Acknowledgements

This work was supported by It's All About Meaningful Employment (IAAME) funds and was performed in association with the Cooper University Hospital (Camden, NJ) as well as the University of Pennsylvania. I would like to thank Jamal Jon Derakhshan, MD, PhD for his multifaceted help. I also would like to thank my advisor Nidhal Bouaynaya, PhD for her guidance and Bradley Ebinger, MS for his support on this project. I also would like to extend my gratitude to my committee Meena Khandelwal, MD for her data and guidance and Ravi Ramachandran, PhD for their insights and interest in my work and his support.

Abstract

Neda Parvin
AUTOMATIC ANALYSIS OF SURFACE ELECTROMYOGRAPHY OF REFLEXES FOR CENTRAL NERVOUS SYSTEM INHIBITION DURING PREGNANCY
2016-2017
Nidhal Bouaynaya, Ph.D.
Master of Science in Electrical and Computer Engineering

Eclampsia is a life-threatening neurological complication (seizures or coma) of pregnancy, and represents progression of pre-eclampsia (high blood pressure and protein in the urine isolated to pregnancy). Even though the exact mechanism of pre-eclampsia and its neurological manifestations have yet to be definitively established, it is known that there is a loss of inhibitory impulses between the cerebral cortex and the spinal cord resulting in exaggerated reflexes. In this work, we establish normative measures for deep tendon reflexes (DTR) during pregnancy. We quantified the surface electromyogram (EMG) at the knee and ankle of DTRs in 279 subjects. The signals were analyzed in the time, frequency and time-frequency domains, including normalization to patient characteristics. We uncovered two new phenomena. The first involves gradual prolongation of the reflex signal (termed latency) throughout pregnancy. The second is that the prolongation of latency is equal in the knee and ankle, allowing the conclusion that the prolongation is due to a delay in signal transduction at the synapse in the spinal cord. This delay likely represents central nervous system inhibition, either due to the effect of upper motor neurons in the spine, but more likely due to an inhibitory cortical effect (possibly hormonal). It is postulated that the quantification of the deep tendon reflex will allow patients with pre-eclampsia to be screened more effectively.

Table of Contents

Abstract v

List of Figures ix

List of Tables xiii

Chapter 1: Introduction 1

1.1 Problem Statement and Background 1

1.2 Summary Literature Review 4

1.3 Research Objectives 5

1.4 Organization 6

Chapter 2: Literature Review 8

2.1 Analyzing EMG Signals 8

2.2 Reflex Latency 9

2.2.1 Emg Onset Detection - Threshold-Based Method. 9

2.2.2 Emg Onset Detection - Wavelet-Based Method. 10

2.3 Amplitude 11

2.3.1 Demodulation. 12

2.3.2 Filtering. 12

2.3.3 Smoothing. 12

Chapter 3: Materials and Methods 14

3.1 Data Acquisition and Preprocessing 14

3.1.1 Importing Data.. 16

3.1.2 Filtering and Pre-Processing 17

3.2 Time Domain Feature: Latency 17

3.2.1 Proposed Algorithm for Onset Detection. 19

Table of Contents (Continued)

3.2.2 Latency Extraction Based on the Mode of Histogram. 20

3.3 Time Domain Feature: Amplitude 22

3.4 Time Domain Feature: Duration 22

3.5 Frequency Domain Analysis 23

3.5.1 Bandwidth. 23

3.5.2 Mean frequency 25

3.6 Time-Frequency Domain Analysis: Discrete Wavelet Transform 25

3.6.1 Total Energy of DWT Coefficients. 28

3.7 Time-Frequency Domain Analysis of Empirical Mode Decomposition 29

3.7.1 Total Energy of IMFs. 30

3.7.2 Mean Frequency of IMFs 30

Chapter 4: Statistical Analysis 33

4.1 Multivariate Linear Regression Model 33

4.2 Tests for Normality 33

4.3 The Analysis of Variance: One -Way ANOVA 34

4.4 The Kruskal-Wallis Test (KW) 35

4.5 Two Sample T-Test 35

Chapter 5: Results 37

5.1 Latency Definition: Peak to First Peak 37

5.2 Comparison of the Right and Left Sides 39

5.3 Mean versus Mode of Latency and Effect of Number of Trials 40

5.4 Normalization of the Latency Based on Age, Height and Weight 42

Table of Contents (Continued)

5.5 Latency and Sexual Dimorphism 44

5.6 Latency and the Phases of Pregnancy 46

5.7 Central Inhibition of DTR Latency 47

5.8 Amplitude Results 49

5.9 Duration Results 49

5.10 Frequency Domain: Bandwidth 51

5.11 Frequency Domain: Mean Frequency 52

5.12 Frequency Domain: Total Energy 52

5.13 Time-Frequency Domain: Total Energy of DWT Coefficients 54

5.14 Time-Frequency Domain: Total Energy of Intrinsic Mode Functions 55

Chapter 6: Discussion 60

Chapter 7: Conclusions and Future Work 67

References 69

List of Figures

Figure Page

Figure 1. Knee reflex measurement, with placement of electrodes and Jendrassik's maneuver, obtained with Taylor hammer and recorded in AcqKnowledge 4.1 software, Biopac Systems Inc, Santa Barbara, CA. 15

Figure 2. Importing data from "AcqKnowledge", Data was imported from a program that captures the EMG signal from the BIOPAK DA100C and EMG100C systems into MATLAB and it was organized into a useful format which separated each hammer tap into left and right knee and ankle categories, and categorized them into pregnancy groups. 17

Figure 3. Definitions of latency and bandwidth, obtained from a surface EMG. It is recorded from the knee of a healthy 33 year-old male volunteer (weight = 68 kg, height = 180 cm). (A) Peak-to-onset. The first arrow and circle denotes the impulse peak, the second arrow denotes the response envelop onset. (B) Peak-to-first peak. (C) Peak-to-peak. (D) Bandwidth was calculated as the width of frequency spectrum at 0.71 max amplitude. 19

Figure 4. Proposed onset detection of a surface EMG, The envelope of the response signal is shown as the blue line. The black line is impulse signal and the green line shows the response signal. The minimum (red arrow) of the signal envelope between impulse artifact and response peaks (*) are calculated. The absolute derivative of the response signal moves forward in time until the mean of moving window is above a threshold. 20

Figure 5. Histogram of the latency results, showing latency results of the ~30 individual trials for a single patient. (A) right knee, (B) right ankle, (C) left knee and (D) left ankle. The mode of the latency was selected for each patient at each location as a method to eliminate outliers, instead of averaging. 21

Figure 6. Amplitude detection, Blue line shows the response signals. The difference between two circles in the blue line indicates the amplitude and the red line shows impulse signal. 22

Figure 7. Duration detection, Green line shows response signals and blue line denotes the envelope of the response signal. There are 4 (x) in the envelope of the response signal. The first one is the onset, second is the first peak, third is the max peak and the last one is the terminal point. Duration is the differences between the onset and terminal point. The terminal point is the point that the average is above the two standard deviation of the noise floor. The floor noise is the terminal portion of the average time reversed response signal. 23

Figure 8. The response signal and the mean frequency of the response signal before and after fatigue, the fatigue increases the low frequency component and decreases the high oscillations in time domain and therefore smaller mean frequency in frequency domain. 25

Figure 9. The four levels of the discrete wavelet coefficients of the response signals are shown as (a_1-a_4) approximations and (d_1-d_4) details. As the level increases the resolotion of the frequancy decreases. 28

Figure 10. Flowchart is depicting the process of EMD. Six IMFs were extracted from the response signal. 30

Figure 11. Instantaneous frequency of intrinsic mode functions (IMF1 and IMF2) as a function of time are shown in A and C. The amplitude of analytic signal of (IMF1 and IMF 2) as a function of time are shown in B and D. 32

Figure 12. Instantaneous frequency of intrinsic mode functions (IMF3 and IMF4) as a function of time are shown in A and C. The amplitude of analytic signal of (IMF3 and IMF 4) as a function of time are shown in B and D. 32

Figure 13. Effect of latency definition. Latency standard deviation (SD) and number of outliers as a function of latency definition in knee and the ankle. 39

Figure 14. Latency as a function of the number of the trials using mode and mean calculations is shown in the black and red lines, respectively for 4 healthy men and 4 healthy women. 41

Figure 15. The cumulative stabilization of the latency as a function of the number of trials shows the percentages of data that reach to the stabilized latency (the point that adding more trials doesn't change the latency) from 166 knee taps and 155 ankle taps (left and right combined) of non-pregnant female and male participants. 41

Figure 16. The dependence of the latency on subject characteristic as a function of (a) age, (b) weight, (c) height and (d) body mass index (BMI). Data is shown for all males as well as non-pregnant females in the knee.....43

Figure 17. The dependence of latency as function of height is shown for both combined and noncombined data. Uncombined sexes (A) and combined sexes (B) in the knee; Uncombined sexes (C) and combined sexes (D) in the ankle. 45

Figure 18. Group-wise latency as a function of pregnancy phase results of the using box and whisker plots. Latency in the (a) knee and (b) ankle as well as normalized latency in the (c) knee and (d) ankle. Group designations are: 1- males, 2- non-pregnant females, 3-first trimester, 4-second trimester, 5-third trimester, 6-term and 7- post-partum. * denotes significant deference with respect to the non-pregnant female group; (+) denotes outlier data. 47

Figure 19. Average latency difference of all groups from the non-pregnant females. The last column represents the average difference of all stages of pregnancy compared to non-pregnant females. Note that the average latency difference throughout pregnancy is similar in the knee and ankle. 48

Figure 20. Change in latency during pregnancy fitted to a line. X denotes the data points and the line is the linear fit. Note the increase in latency during pregnancy. The error bars represent standard deviation at each observation point. 49

Figure 21. Duration results in the knee (a) and ankle (b) of the response signal for all groups. The group designations are the same as prior figures. 50

Figure 22. The bandwidth, mean frequency and total energy results of the response signal for various groups. Signal bandwidth in the (A) knee and (B) ankle. Mean frequency in the knee(C) and ankle (D). Total energy in the knee (E) and ankle (F). Group designations are: 1- males, 2- non-pregnant females, 3-first trimester, 4-second trimester, 5-third trimester, 6-term and 7- post-partum.....53

Figure 23. Total energy results of first three levels of the DWT coefficients are shown for all groups. Group designations are: 1- males, 2- non-pregnant females, 3-first trimester, 4-second trimester, 5-third trimester, 6-term and 7- post-partum. 55

Figure 24. Total energy results of first and second IMFs of EMD are shown for all groups. Group designations are: 1- males, 2- non-pregnant females, 3-first trimester, 4-second trimester, 5-third trimester, 6-term and 7- post-partum. Time-Frequency Domain: Mean Frequency of IMFs 56

Figure 25. Mean frequency (MNF) results of first (A&B) and second IMFs (C&D) of EMD are shown all various groups. Group designations are: 1- males, 2- non-pregnant females, 3-first trimester, 4-second trimester, 5-third trimester, 6-term and 7- post-partum. 57

List of Tables

Table Page

Table 1. Participant Characteristics, by Group (N = 279 Healthy Volunteers).....38

Table 2. Paired Sample T-Test for Left and Right Knee.....40

Table 3. The Multiple Linear Regression Coefficients for Combined Men and Women. 43

Table 4. Revised Multiple Linear Regression Coefficients for Men and Non-Pregnant Women Fitted Separately. 45

Table 5. Subjects' Time-Domain Features and Their Confidence Intervals, By Group.....50

Table 6. Subjects' Frequency Domain Features and Their Confidence Intervals, By Group. 53

Table 7. Subjects' Time-Frequency Domain (DWT) Features and Their Confidence Intervals, By Group.....58

Table 8. Subjects' Time- Frequency Domain (Imfs) Features and Their Confidence Intervals, By Group.....59

Chapter 1

Introduction

In this section, we will motivate and state the problem of pre-eclampsia and eclampsia in pregnancy. An important predictive marker for progression to eclampsia (seizures) is hyperreflexia. However, assessment of deep tendon reflexes (DTR) – used to measure hyperreflexia – is subjective and therefore shows variability. We will review all approaches applied in this field and shed the light on the main contributions of our thesis work.

1.1 Problem Statement and Background

Pre-eclampsia is a unique complication of human pregnancy. Clinically, pre-eclampsia is defined as gestational hypertension (i.e. hypertension detected for the first time after 20 weeks of gestation) along with proteinuria (300 mg or more protein in urine per 24 hour period) in at least two random urine samples collected at least 6 hours apart [1]. Pre-eclampsia may progress to include neurological symptoms (seizures) and is life threatening. The current hypothesis presumes that irritability of the central nervous system (CNS) occurs secondary to vasospasm or cerebral edema [2]. Even though the exact mechanism of pre-eclampsia and its neurological manifestations have yet to be definitively established, it is known that there is a loss of inhibitory impulses between the cerebral cortex and the spinal cord resulting in exaggerated reflexes [3]. Witlin *et al.* showed that headache and hyperreflexia were the most important predictors for occurrence of seizures in women with pre-eclampsia [3]. Hyperreflexia suggests irritability of the Central Nervous System (CNS), which is a risk factor for seizures. Seizures in pregnancy can result in significant maternal and fetal morbidity and mortality

[4]. Therefore, seizure prophylaxis with magnesium (Mg) is used in all patients with pre-eclampsia. Recently, however, there has been a debate regarding the use of Mg for seizure prophylaxis in all women with pre-eclampsia. Some have advocated its use only in women with severe gestational hypertension due to significant side effects and low therapeutic index [5], [6]. The incidence of eclampsia in women with severe pre-eclampsia is only ~2%, whereas the number of patients needed to treat (NNT) to prevent 1 case of eclampsia varies from 36 to 385. Occurrence of eclampsia is currently unpredictable and only sometimes depends on disease severity [4].

The elucidation and assessment of deep tendon reflexes (DTR) represents one of the main components of the clinical examination of the nervous system. The assessment of DTRs, a first step in the neurological diagnostic process, provides information on the integrity of the central as well as peripheral nervous system. A reflex arc is comprised of stimulation of a muscle spindle, conduction in peripheral sensory (afferent) nerve, synapse in the spinal cord, conduction in an efferent motor nerve and contraction of a muscle. The synapse in the spine is modulated by upper motor neurons, descending from the brain and connecting in the anterior horn of the spinal cord. Therefore, a deep tendon reflex interrogates information from both peripheral and central nervous systems. Each muscle in the body contains a small sensory unit called a muscle spindle, which controls muscle tone and detects changes in the length of the main muscle fibers. When a tendon is tapped with a reflex hammer, the muscle stretches, lengthening the spindle and the bulk of the muscle fibers. The spindle then stimulates a sensory nerve, which reaches the spine to synapse in the anterior horn of the spinal cord. There the signal stimulates the efferent

neuron or motor pathway to contract the muscle. As the muscle contracts, the spindle shortens and stops firing [7].

One of the main significances of the tendon reflex response is its sensitivity for detecting inhibiting and facilitating influences from the brain. A cortical or spinal cord lesion above the level of the reflex disrupts the equilibrium of impulses between the cerebral cortex and the spinal cord preventing the cortex from transmitting inhibitory impulses to the spinal cord. When the spinal cord synapse does not receive sufficient restraint from the cerebral cortex, the reflex arc is uninhibited, causing hyperreflexia. The DTR also probes the peripheral nervous system (PNS); if the upper motor neuron pathway is intact but the lower motor neuron (i.e. peripheral nerve) is disrupted, then hyperreflexia occurs. Clinically, reflexes are elicited and graded subjectively as absent (0), decreased in amplitude (1+), normal (2+), increased in amplitude (3+) or failing to stop (clonus, 4+). Therefore, one hypothesis of this work is that quantitative analysis of reflexes will allow more accurate quantitative assessment of both reflex magnitude as well as measuring reflex signal duration and latency, which is not able to be measured by a clinician since they are on the millisecond order, adding additional critically important dimensions.

We also hypothesize that patients with pre-eclampsia who progress to eclampsia will have changes observable in the reflex arc and thereby we might predict patients at risk for progressing, allowing fewer patients to be pre-treated with magnesium. However, before examining this hypothesis, we first need to establish normative measures for DTRs during pregnancy.

1.2 Summary Literature Review

Measuring DTR response using surface EMG may give a quick and easy bedside evaluation of the patient. Current practice evaluates DTRs subjectively with a large inter-observer variability [8], [9]. The National Institute of Neurological Disorders and Stroke (NINDS), a division of the National Institutes of Health (NIH), developed a scale, published in the early 1990's and measured on a 0 to 4 scale [10]. Manschot and colleagues [8] found that neither the Mayo nor the NINDS scale performs sufficiently well with different observers, as denoted by poor inter-observer agreement coefficient (k=0.35). Similarly, Stam *et al* [9]showed considerable inter-observer disagreement with clinical examination of tendon reflexes, even on the subject of asymmetry. Litvak *et al* [11]showed that training did not improve the reliability of the NINDS scale. Considering the significant variability with subjective methods, objective quantification of DTRs seems to be a more logical step. Dietrichson and Sorbye [12] in 1971 first showed the electric recording of the ankle reflex. Stam *et al* [13]showed in 1984 that electromyography (EMG) recordings can be used as a valid measure of reflex amplitude, and clinically apparent reflex asymmetry can be reproduced and documented. Since then several investigators have attempted to establish reliable, quantifiable, and reproducible measures of DTR assessment and interpretations [14], [15], [16], [17], [18], [19]. However, the number of subjects enrolled has been small, with a wide age range (from 2 days of age to 80 years old), and with very few women in the study group. In addition, and most significantly, no pregnant females were enrolled.

The parameter with greatest reproducibility consistently has been the DTR latency defined as the time elapsed between the tendon tap stimulus and the first deflection from

the recorded signal. There is considerable disagreement between other parameters like amplitude and duration of response of the DTR signal. Therefore, we believe that there is a significant and unmet need to develop accurate measures to *objectively* quantify DTRs in normal pregnant women. To date, there are nine publications on normotensive electromyography data of the patellar reflex [14], [15], [16], [18], [20], [21], [22], [23], [24], but only one of them was conducted during pregnancy[22]. This single study in pregnancy showed no significant change in latency during pregnancy; however, their sample size was smaller than ours (208 vs. 218), their number of taps per patient was 3 times smaller than ours (10 vs. 30), and their reflexes were measured only in the knee whereas in this study, measurements were made at both the knee and ankle.

1.3 Research Objectives

This work is the first study, which considers normotensive electromyography data of both the ankle and knee reflexes in pregnant females, non-pregnant females and men. This work is also the first research that compares latency in knee and ankle in normotensive pregnant women. The main research objectives of this work include:

1. to derive a non-invasive quantitative methodology to objectively measure DTR response;
2. to establish normal parameters for DTRs in pregnancy (latency, amplitude and bandwidth);
3. to determine whether DTR parameters vary by stage of pregnancy;
4. to compare the differences of the DTR parameters between males and females;

5. to examine the main reason of DTR delay (or prolonged latency); namely is it related to nerve conduction velocity or is it related to a central inhibition of the reflex arc at the level of the spinal cord.

1.4 Organization

This thesis is organized as follows:

In chapter 2, we elaborate on the literature review of mathematical quantification of deep tendon reflexes in time, frequency and time-frequency domains. It is crucial to consider previous studies in order to select the best features that show more deference between the groups (males, non-pregnant females, four stages of pregnancy and post-partum).

In chapter 3, we introduce our proposed materials and methods, including data collection, denoising, and analysis in time, frequency and time-frequency domains.

In Chapter 4, we review statistical analysis, including single factor ANOVA, Kruskal test with 7 levels to determine whether there are significant differences among the 7 sub-cohorts and t-test to determine the deference between left and right knee and ankle. Then, we review multivariate linear regression to normalize the latency with respect to height, weight and age.

In Chapter 5, we provide our results in time domain, frequency domain and time frequency domain.

In Chapter 6, we discuss and compare our results with previous studies [22]. We also discuss the main reason of delay (latency), namely is it due to nerve conduction velocity or is it related to a central inhibition of the reflex arc at the level of the spinal cord.

Finally, in Chapter 7, we provide a brief conclusion that summarizes the main findings of this thesis.

Chapter 2

Literature Review

In this chapter, we will review previous work in analyzing the surface electromyography signals and show the effect of different noise in the EMG signals and provide strategies for elimination or reduction. Then, we will review feature extraction and signal processing techniques for deep tendon reflexes.

2.1 Analyzing EMG Signals

Electromyography is the recording of the electrical signal that emanates from contracting muscles. From a medical perspective understanding the precise value of the response time is very important. That is why we are interested in measuring the initiation time or the first inflection point of the response signal of the EMG signal. Then, we will report the signal parameters used to measure the amplitude of the reflex. In order to precisely extract the features from the signals we need to detect the noise in the signal and eliminate their influences. DeLuca *et al.* [25] showed that extrinsic and intrinsic factors, which are associated with the electrode structure and its placement on the surface of the skin above the muscle, can greatly influence the signal detected. Intrinsic factors are due to physiological and biochemical characteristics of the muscle. For instance, the number of active motor units can affect signal amplitude and duration; the fiber diameter, which can influence amplitude and conduction velocity; and the depth of tissue (skin and adipose) between the electrodes and the muscle, which affects spatial filtering. Extrinsic factors are usually under control of the researcher and are related to electrode configuration, which can significantly influence the quality and quantity of the detected signal. For example, the area and shape of the electrodes and their position over the

muscle can have a significant impact on the reflex signal [25].

2.2 Reflex Latency

In this section, we provide signal processing methods that are used to extract the features of deep tendon reflexes. To the best of our knowledge, all the literature that quantified deep tendon reflexes in the time-domain relied on two features: reflex latency and amplitude.

Many studies of quantification of deep tendon reflexes defined the reflex latency as the time between the hammer strike and the onset of muscle activity [13], [20], [26], [22], [27], [28]. Frinjns and Laman measured latencies from stimulus to the first negative deflection from the baseline [15]. The mathematical model and the methods used for onset detection were not clearly articulated. Onset detection of muscle activity has been a topic of investigation for many years in surface EMG signal processing for various applications. In what follows we review the numerous methods for surface EMG onset detection.

2.2.1 Emg onset detection - Threshold-based method. Hodges and Bui [29] introduced a threshold based method for onset detection of EMG signals. The mean μ and standard deviation σ of the baseline for each reference signal were computed. The threshold T was computed as:

$$T = \mu + h\sigma, \qquad (2\text{-}1)$$

where h is the level of the threshold [30]. The estimated onset time t_1 was identified as the first point when the smoothed signal exceeded the threshold T for more than 25 consecutive samples [31]. Stanisław Solnik *et.al* showed that Teager-Kaiser Energy

Operator (TKEO) [30] can increase the accuracy of onset detection in EMG signal. The discrete TKEO was defined as:

$$\Psi\,[x(n)] = x^2(n) - x(n+1)x(n-1), \qquad (2\text{-}2)$$

where x is the EMG signal and n is the sample number. Different threshold levels were set and it has been shown that the threshold level T=15 was the most robust with respect to high baseline noise and low amplitude of recorded EMG signals and has the smallest detection errors [31]. However, its performance may be compromised by low SNRs (defined as the sample mean of the EMG signal divided by its standard deviation) of the surface EMG considering that the signal amplitude is sensitive to all sorts of noise.

2.2.2 Emg onset detection - wavelet-based method. Merlo *et al* [32] proposed a wavelet-based method to determine the onset of the muscle activity in EMG signals. They modeled the EMG signal as the sum of muscle unit action potential trains (MUAPT). The $\boldsymbol{j^{th}}$MUAPT is defined as:

$$MUAPT_j(t) = \sum_i k_j \,.\, f\left(\frac{t-\theta_{ij}}{\alpha_j}\right) \qquad (2\text{-}3)$$

where j is the specific MU(smallest controllable unit of the muscle), k is an amplitude factor, f is a prototype function, θ_{ij} is the occurrence time of the MUAPs of the MU and α_j is a scaling factor [32]. The MUAP is the conduction of an electrical potential in a muscle fiber as a result of the recruitment of the MU [33]. The EMG signal is modeled by the sum of MUAPs and adaptive noise. In this model, the authors assumed that the different MUAPs have the same shape but different width and amplitude. The Continuous wavelet transform (CWT) is defined as:

$$CWT(a,\tau) = \int_{-\infty}^{+\infty} S(t)\,.\,W^*\left(\frac{t-\tau}{a}\right)\,dt, \quad (2\text{-}4)$$

where $S(t)$ is the EMG signal, which will be estimated by the mother wavelet $w(t)$. τ is the translation index and a is a scaling parameter. The high coefficients indicate a high similarity to the finite shape of the wavelet. As a result, the peaks in wavelet coefficients identify changes from inactivity to activity.[32] Analysis was done with a wavelet design based on the Hermite– Rodriguez (HR) function to describe the basic MUAP shape.

$$HR_1(t) = k_{n,1}.H_1\left(\frac{t}{\lambda_n}\right)e^{\frac{e^{-t^2}}{\lambda n^2}}, \quad (2\text{-}5)$$

where n is the scale factor, $k_{n,1}$ is a normalization factor, $HR_1(t)$ is the Hermite polynomial of order one [32], and $\lambda_n$indicates the function duration. Standard Daubechies order 6 is chosen as a mother wavelet in order to obtain wavelet durations within the physiological MUAP durations (5–40 ms). After decomposing the simulated and noise signals with CWT, operations were done on the maximum coefficients. He defined the $\eta(t)$ function and the threshold of the $\eta(t)$ within the interval that EMG activity is not presented.

$$\eta(t) = \max\{CWT(\alpha, t)\}, \quad (2\text{-}6)$$

$$M = \max\{\eta(t)\} \quad 0 < t < T_{noise}, \quad (2\text{-}7)$$

$$th = \gamma.M, \quad (2\text{-}8)$$

where γ is a constant multiplier. The point that reaches above the threshold indicates the onset of the signal.

2.3 Amplitude

The amplitude is considered an important feature of the EMG signal because of a possible relationship between the amplitude and the discharge rate of the active motor unit [34]. The amplitude of deep tendon reflexes has been calculated by many investigators as the difference between the maximum and the minimum of the response

signal [15], [22]. The preprocessing stages should be performed before calculating the amplitude value e.g. demodulation [35] , filtering and smoothing [36].

2.3.1 Demodulation. The EMG amplitude was treated as a zero mean by early investigator [35]. Inman *et al*. [35] suggested demodulation by getting the first-power (or absolute value) of the signal. Hogan and Mann [37] showed that the second-power (or RMS) demodulator would give the best maximum likelihood estimate of the EMG amplitude for constant force.

2.3.2 Filtering. There are various sources of EMG measurement noise (extrinsic factors) e.g. the electrode noise, the electrode motion artifact, the cable motion artifact, and the alternating current power line interference. The electrode noise is related to electrode impedance. Electrode impedance depends on electrode size, the signal frequency and the current density. By minimizing the electrode–skin impedance and using a signal amplifier, this problem can be reduced. The mechanical disturbance of the electrode charge layer and deformation of the skin under the electrodes is the electrode motion artifact and it is due to the relative movement between the electrode and the underlying skin. The power density of motion artifact is mostly below 20 Hz, so this problem can be reduce by using high pass filter with a cut-off frequency at 20 Hz [38]. Since the frequency of the AC power supply is 60 Hz in North America (and 50 Hz in Europe), the power line noise can be removed by using the 60 Hz Notch filter.

2.3.3 Smoothing. There exist two common signal processing techniques to smooth the measured reflex signal: 1) Root mean square smoothing; 2) Signal averaging. Basmajian and DeLuca [36] used root mean square to smooth the EMG signal. The root mean square is computed by squaring each data point, summing the squares, dividing the

sum by observations, and taking the square root over chosen time intervals or windows, which are defined by user. Longer windows result in fewer data points, and a smoother signal, [36]. This method filters the signal to provide a more general representation of muscular activity, [36].

In signal averaging, multiple trials are superimposed on one another to create a signal that represents all trials' activity [36]. However, in order to use signal averaging, data must be acquired at the same precise time and duration across all trials. This can be accomplished through a trigger-sweep data-collection mode using a mechanically reliable triggering device to clearly define when a trial begins and ends, [36].

Chapter 3

Materials and Methods

In this chapter, we first describe our data acquisition and preprocessing techniques. Then, we describe our proposed definition of latency and our proposed method for onset detection as well as other features in the frequency and time- frequency domains.

3.1 Data Acquisition and Preprocessing

Deep tendon reflex of the knee and ankle was recorded prospectively in 279 healthy subjects aged 15-45 years in this study. 21 women in the first trimester (defined as from beginning of gestation to 14 weeks and 6 days), 48 in the 2nd trimester (end of first trimester to 15-27 weeks and 6 days), 42 in the 3rd trimester (defined as end of second trimester to 28-36 weeks and 6 days), 25 at term (defined as 37 to 42 weeks), 51 at day 1 -3 postpartum, 47 non pregnant women, and 45 men. The study was approved by the local IRB. The participants' characteristics per group, in terms of age, height, weight and BMI are shown in Table 1. The reflexes were recorded with a forced transducer (Biopac MP-150 Analog-Digital System, Biopac Systems Inc., Santa Barbara CA). A Taylor hammer was used for all recordings. Surface electrodes were the standard Ag/AgCl electrodes (6.5mm in diameter). The subject was in a relaxed and sitting position with bare legs hanging off the edge of the bed. To assess the knee reflex, the reference electrode was placed just above the patella, and the recording electrode was placed 10 cm above it over the rectus muscle. All patients were instructed to perform the Jendrassik's maneuver by locking the fingers and attempt to pull apart the hands forcefully Figure 1. This method has been used by other authors [15], [21], [22]. Ground

electrodes were placed medial to the joints. Recordings were made on both extremities. Care was taken to direct it at right angles the tendon. As joint positions may interfere with tendon response latencies, joints were kept in normalized position, i.e. knee at about 90 degrees. Each tendon was tapped 30 times, each tap separated by 10 seconds. Before starting measurements, subjects were instructed to interrupt the experiment if they experience any discomfort. Auditory feedback was provided to subjects with difficulty relaxing during DTR recording. For the ankle reflex, the reference electrode was placed proximal to the Achilles tendon while the recording electrode was placed over the gastrocnemius muscle between the midpoint of the popliteal fossa and upper border of medial malleolus.

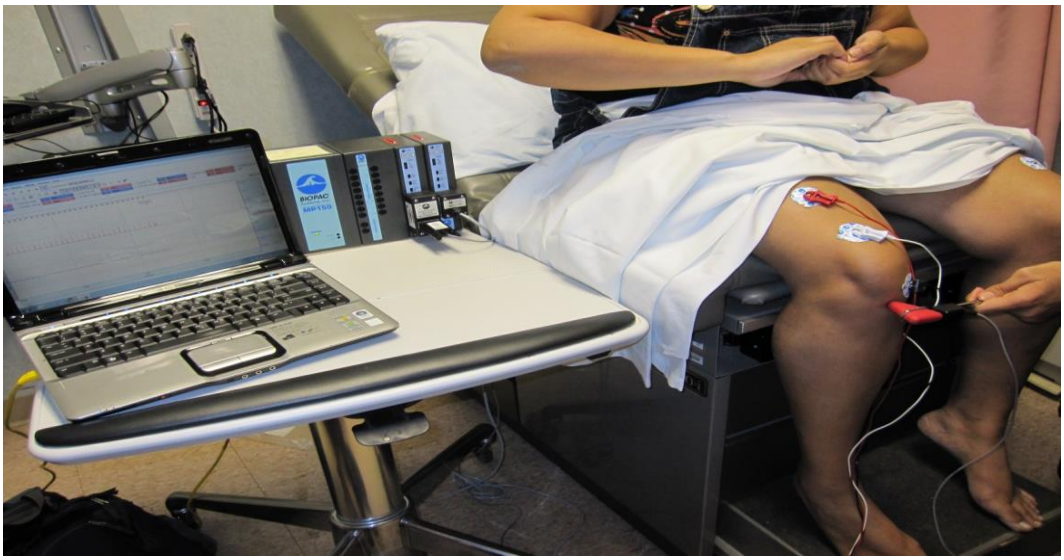

Figure 1. Knee reflex measurement, with placement of electrodes and Jendrassik's maneuver, obtained with Taylor hammer and recorded in AcqKnowledge 4.1 software, Biopac Systems Inc, Santa Barbara, CA.

3.1.1 Importing data. The script being used was only able to read an older version of the .acq files. Because of this, each of the .acq files had to be reopened and saved in another, more readable format. The parsing script could not read the flags that were put into the program, so the files also had to be separated into 4 separate files (left knee, right knee, left ankle, right ankle). This was very time consuming. A newer version of the same script was found that could import the newer version of the .acq files. By looking at the save file itself using a hex editor and referencing the parsing script that was being used to import the .acq file, the structure was found that holds the flag events in the save file. This was used to extend the parsing script in MATLAB to support the import of events and flags. By using this new extension, the position of the flag was able to be calculated, which eliminated the need for four files and the conversion to the older .acq file type Figure 2.

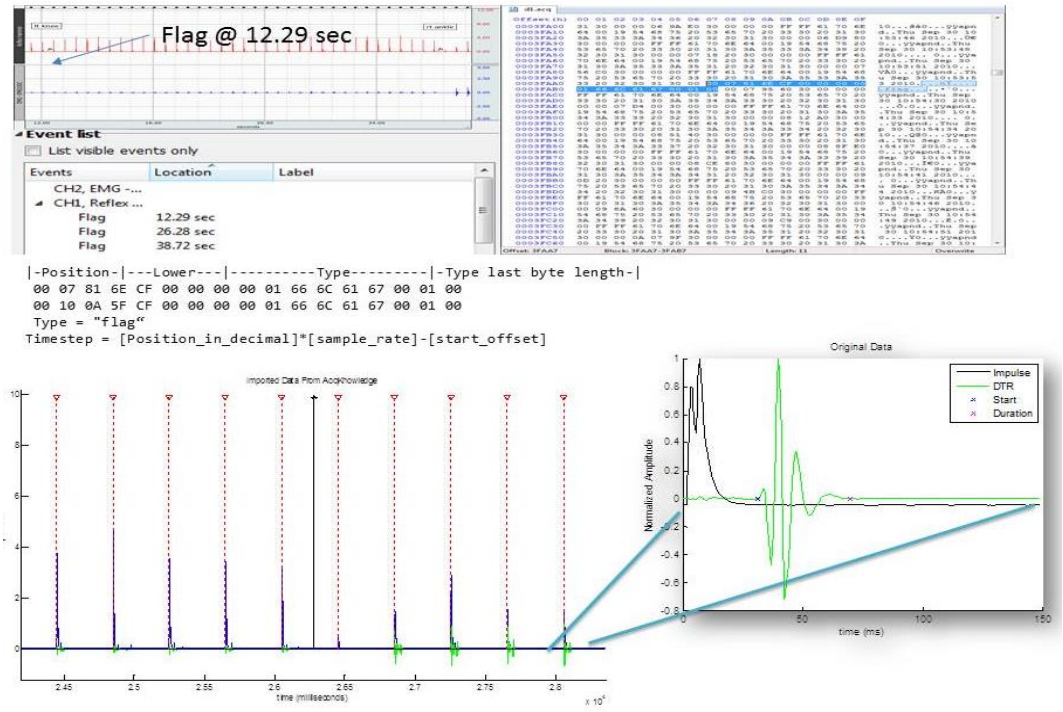

Figure 2. Importing data from "AcqKnowledge", Data was imported from a program that captures the EMG signal from the BIOPAK DA100C and EMG100C systems into MATLAB and it was organized into a useful format which separated each hammer tap into left and right knee and ankle categories, and categorized them into pregnancy groups.

3.1.2 Filtering and pre-processing. All biological signals are prone to noise, necessitating certain preprocessing denoising steps as was discussed in chapter 2. All EMG signals were first filtered by a notch filter (59-61 Hz) to reduce line noise, followed by a 500 Hz low pass filter to remove any high frequency artifacts. Baseline removal was applied (by high pass filtering) to each recording to eliminate drift that may be induced by the measurement device or otherwise. The EMG signals were sampled at 1250 Hz (.8 ms/sample).

3.2 Time Domain Feature: Latency

The muscle response time, also called *latency*, can be defined in several ways, as illustrated in Figure 3 shows the impulse signal and the DTR response signal from a

surface EMG in the knee of a healthy man. The envelope of the response signal was calculated, which is a smooth curve outlining its local maximums [39]. The arrows in Figure 3-a, 3-b, 3-c show the peak-to-onset, peak-to-first-peak, and peak-to-peak possible definitions of latency, respectively.

We created an onset detection algorithm based on the sign changes of the Hilbert transform of the response signal. We measured the definition of latency that is most robust to the 30 tap trials, e.g. the definition that leads to the minimum number of outliers among the 30 trials for each subject. The group standard deviation of latency was also compared using the three definitions as a second metric. We found that the most robust characterization of latency is the peak-to-first-peak definition (least number of outliers and lower group standard deviation). We therefore adopted this definition of the DTR latency. Previous studies have shown that the EMG amplitude is attenuated, influencing the ability to detect the onset of muscle activity [40]. The reduction in the signal amplitude may be due to the overlap of opposing phases of individual motor unit action potentials [41], [42]. Therefore, finding the true onset of the signal is not always accurate.

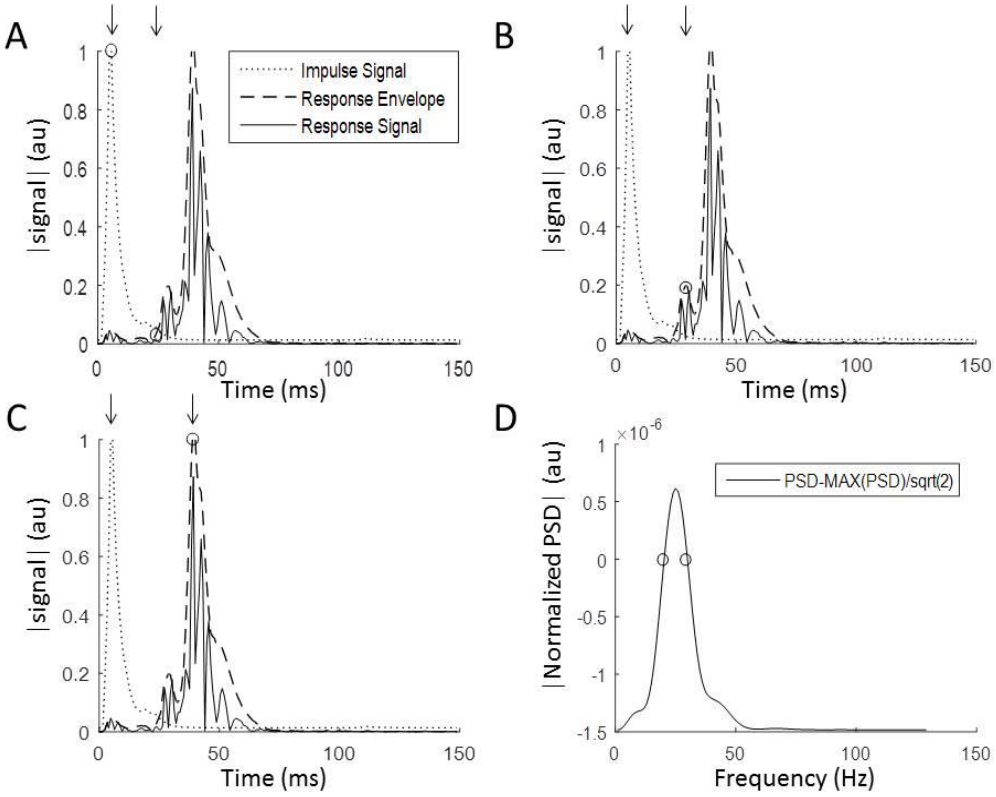

Figure 3. Definitions of latency and bandwidth, obtained from a surface EMG. It is recorded from the knee of a healthy 33 year-old male volunteer (weight = 68 kg, height = 180 cm). (A) Peak-to-onset. The first arrow and circle denotes the impulse peak, the second arrow denotes the response envelop onset. (B) Peak-to-first peak. (C) Peak-to-peak. (D) Bandwidth was calculated as the width of frequency spectrum at 0.71 max amplitude.

3.2.1 Proposed algorithm for onset detection. The reflex signal $\boldsymbol{s(t)}$ is modeled by the superposition of some damped sinusoidal wave representing impulse artifacts $\boldsymbol{i(t)}$ and the true response signal $\boldsymbol{r(t)}$, plus noise($\boldsymbol{t}$):

$$s(t) = i(t) + r(t) + n(t) \quad (3\text{-}1)$$

The point in which the response signal's envelope hits a minimum indicates a point where the response signal's impulse artifacts have dropped off and is an ideal spot to start windowing the absolute value of derivative of the response signal until a change in the signal rate increase above the threshold. The threshold is usually based on the noise

level before reflex elicitation or the maximum voluntary contraction signal. Taking the local minimum of the signal envelope (using Hilbert Transform) between the impulse peak and the response signal peak provides a good starting point to start a moving window. This moving window moves forward in time along the signal until its mean is above a threshold (Figure 4).

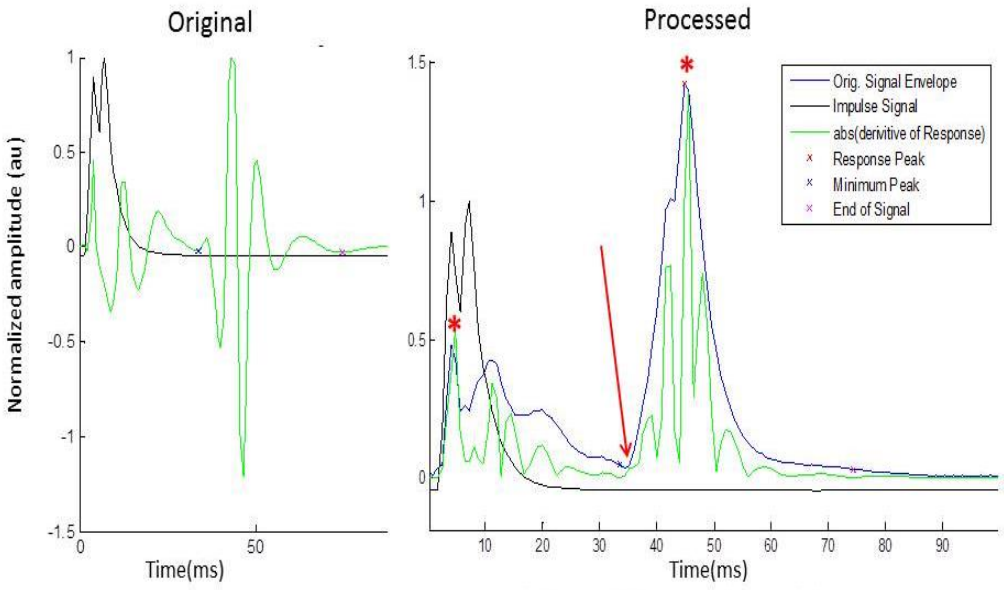

Figure 4. Proposed onset detection of a surface EMG, The envelope of the response signal is shown as the blue line. The black line is impulse signal and the green line shows the response signal. The minimum (red arrow) of the signal envelope between impulse artifact and response peaks (*) are calculated. The absolute derivative of the response signal moves forward in time until the mean of moving window is above a threshold.

3.2.2 Latency extraction based on the mode of histogram. The first peak time was found by doing a peak search for maximum values in the impulse signal and returning the index at which the first peak was detected. This was done assuming the first peak was the actual impulse and the rest are artifacts from the reflex hammer that can be ignored. The response peak time was found by doing a peak search for

maximum values in the envelope of the response signal and returning the index at which the first peak of the response envelope was detected. This process was done for 30 hammer tap trials. The histogram of each trial was plotted and the mode of trials was selected as shown in Figure 5. Some studies suggested that there may be attrition in the DTR response over time after a number of taps, referred to as 'reflex decay' [20], [43]. We propose to select the mode of the latency for each subject at each location (knee or ankle) as a method to eliminate outliers, as well as to eliminate any changes due to reflex decay. The rationale behind selecting the mode latency of the trials compared to the mean is that, unlike the mean, the mode does not take into account outliers. In summary, the latency of the DTR of every subject is calculated as the mode of the latency values corresponding to the 30 tap trials for that subject, and computed according to the peak-to-first-peak definition.

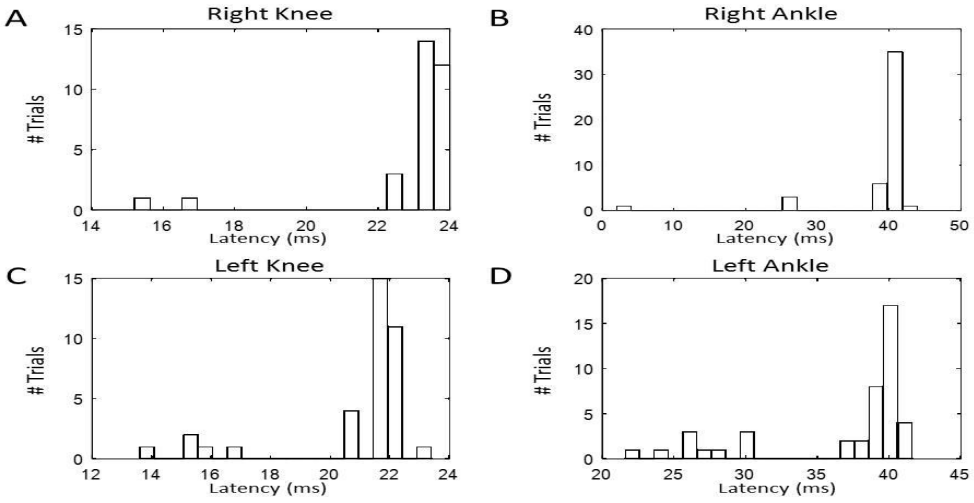

Figure 5. Histogram of the latency results, showing latency results of the ~30 individual trials for a single patient. (A) right knee, (B) right ankle, (C) left knee and (D) left ankle. The mode of the latency was selected for each patient at each location as a method to eliminate outliers, instead of averaging.

3.3 Time Domain Feature: Amplitude

In addition to the *latency*, we defined the *amplitude* as the difference between the maximum and the minimum of the response signal (Figure 6). It has been argued that, since reflex amplitudes show a large inter- and intra-individual variability, they are less useful in characterizing the DTR signal [15], [44], [20].

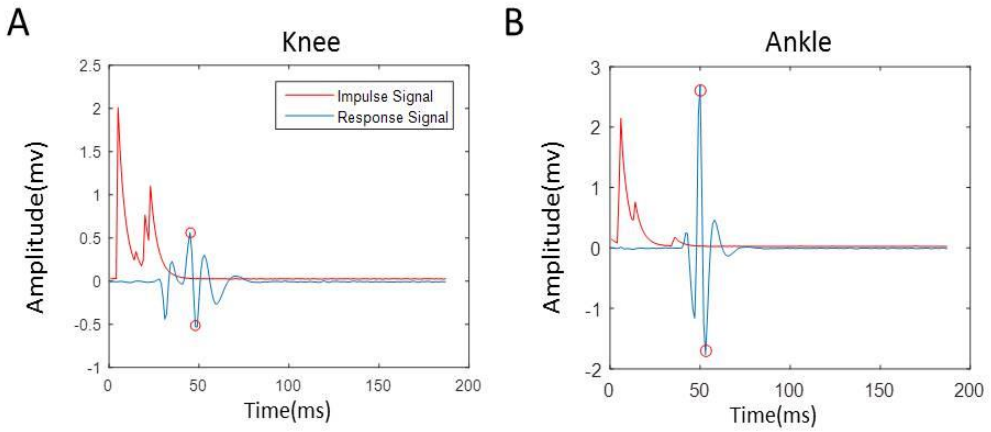

Figure 6. Amplitude detection, Blue line shows the response signals. The difference between two circles in the blue line indicates the amplitude and the red line shows impulse signal.

3.4 Time Domain Feature: Duration

Duration time is the difference between the onset of the first inflection point and the terminal point, where the signal's envelope moves below a threshold. The inflection has already been determined during the latency detection. The terminal point was determined by moving forward in time using a sliding window, starting the last peak of the response signal, and stop when the envelope of the signal has moved below a threshold. The threshold ("noise floor") was chosen as two times of the maximum standard division of the time reverse response signal over a 45ms interval (Figure 7).

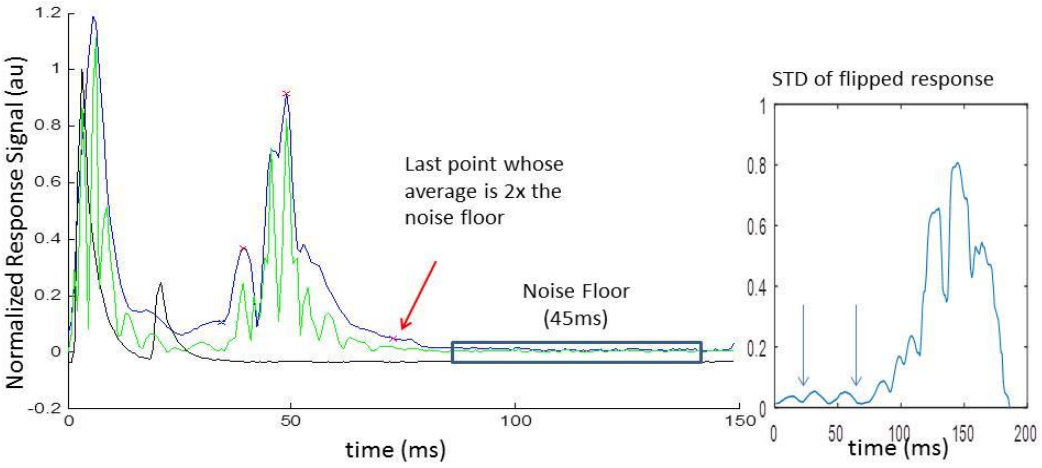

Figure 7. Duration detection, Green line shows response signals and blue line denotes the envelope of the response signal. There are 4 (x) in the envelope of the response signal. The first one is the onset, second is the first peak, third is the max peak and the last one is the terminal point. Duration is the differences between the onset and terminal point. The terminal point is the point that the average is above the two standard deviation of the noise floor. The floor noise is the terminal portion of the average time reversed response signal.

3.5 Frequency Domain Analysis

Spectral content of the EMG often provides important information not readily available in the original time domain signal, as spectral analysis allows decomposition of complex time-domain signals into frequency components, which can be further analyzed. In order to determine whether there are differences in the spectral content of the signals from different cohorts, we used standard frequency domain techniques, such as Welch's method for spectral estimation. Three features were extracted from the power spectrum density of the signals and analyzed for the left and right knee and ankle.

3.5.1 Bandwidth. In addition to the time-domain features **(**latency, amplitude and duration) of the response signal, we also considered a frequency-domain characterization of the signal. Specifically, we use the bandwidth (BW) of the power

spectrum as an additional feature. The power spectrum of a signal describes the distribution of power (or energy) into the frequency components that compose the signal. For instance, the power spectrum of a (finite-sample) pure tone signal will be concentrated around the unique frequency of the tone and show almost zero power in other frequency bands. A key characterization of the power spectrum is its bandwidth, which refers to the frequency range (in hertz) that carries most of the energy in the signal. Figure 3-d shows the spectrum of a DTR signal, where the x-axis displays the frequencies present in the signal and the y-axis displays the normalized energy (with respect to the mean). Although PSD can be estimated by different methods, i.e. non-parametric or model-based, the most commonly used PSD estimator in the EMG signal analysis is the Periodogram. It is defined as the square of absolute value of the Fourier transform of EMG signal divided by the signal length:

$$p_x\left(e^{jw}\right) = \sum_{-N+1}^{N-1} r_x\,(k)e^{-jkw}, \quad (3\text{-}2)$$

$$r_x(k) = \frac{1}{N}\sum_{k=0}^{N-1-k} x(n+k)x^*(n) \quad k = 0,1\ldots,N-1, \quad (3\text{-}3)$$

where $r_x(k)$ is the autocorrelation sequence. An FFT-based power spectral density (PSD) analysis was performed with the Matlab software using Welch's algorithm with Hamming window of length 256 and 50% overlap between segments. Welch's method shows significant reduction of variation in the power spectrum density estimator compared with the periodogram, as it gives an averaged periodogram. In our work, the Matlab script *"pwelch"* was used with the parameter settings to estimate the PSD [45]. The bandwidth of the response signals are shown in Figure. 3-d.

3.5.2 Mean frequency. The Mean Frequency (MNF) of the signal is described as a weighted average frequency [46].

$$MNF = \frac{\sum_{i=1}^{m} f_i p_i}{\sum_{i=1}^{m} p_i}, \qquad (3\text{-}4)$$

where p_i is the power value corresponding to the frequency f_i , and m is the length of the frequency bin. The MNF of surface electromyography (EMG) signal is an important index of muscle fatigue. The reduction in the maximum tension that the person can produce is fatigue. Fatigue is shown as an increase in the amplitude of the low frequency band and a relative decrease in the higher frequencies. That is why the spectral parameter derived from the EMG signal, such as mean frequency (MNF), is frequently used to track muscular changes. (Figure 8)

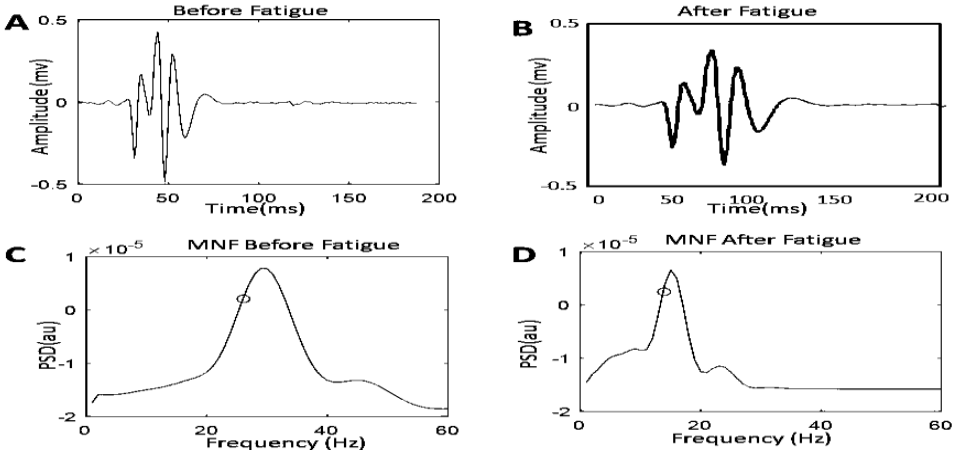

Figure 8. The response signal and the mean frequency of the response signal before and after fatigue, the fatigue increases the low frequency component and decreases the high oscillations in time domain and therefore smaller mean frequency in frequency domain.

3.6 Time-Frequency Domain Analysis: Discrete Wavelet Transform

The spectral estimation techniques are routinely used in analysis of biological signals. However, a primary assumption made by such techniques, limits the amount of

information that can be extracted. Specifically, frequency domain approaches assume that the signal is stationary, that is, its spectral content does not change in time. This assumption is not true for biomedical signals in general and EMG signals, in particular. As such, spectral methods can help us answer the question "what spectral (frequency) components exist in the signal?", but they cannot answer the question "in what time intervals certain frequency components appear?" To answer such a question, we need to use a joint time-frequency representation, which analyzes the signal both in time and frequency domains simultaneously. Considering that the EMG may be a non-stationary signal, and that we are interested in temporal properties of the reflex, a joint time-frequency analysis is not only appropriate but also necessary. We used discrete wavelet transform (DWT) and Empirical Mode Decomposition (EMD) to analyze localized and time-dependent signal energy and power in different frequency bands. A similar ANOVA analysis was used on the features obtained from the DWT and EMD decomposed signal.

DWT iteratively transforms the selected signal into multi-level resolution subsets of coefficients. The DWT transforms the EMG signal with a suitable wavelet prototype, called the mother wavelet. The Discrete Wavelet Transform (DWT) of the signal, $x[n]$, is defined as [47]:

$$X\,[a\,,b\,] = \sum_{n=-\infty}^{\infty} x[n]\varphi_{a,b}\,[\mathrm{n}], \quad (3\text{-}5)$$

$$\varphi_{a,b}[n] = \left(\frac{1}{\sqrt{a}}\right) \times \varphi\left(\frac{n-b}{a}\right), \quad (3\text{-}6)$$

where a represents the scale parameter, b represents the translation parameter (time shifting), $\varphi_{a,b}[n]$ is the basis function which is the scaled mother wavelet. For analysis of

the low-frequency components of the signal a is large and the basis function is stretched. Also a small a contracts the basis function, which is useful for the analysis of the high-frequency components of the signal. The total power spectrum density was obtained for each level. Each band of frequencies for each level is half of the previous level of sample frequency. The maximum frequency of the signal based on Nyquist theorem is: $f_{max} = \frac{\text{sampling frequancy}}{2}$ to prevent aliasing. The first level bandwidth is $\frac{f_{max}}{2}$ to f_{max} (i.e. 312-625 HZ) , second level is 156-312Hz, third level is 78-156Hz and the fourth level is 39-78Hz. Because of the similarity of Daubechies to the motor unit action potential (MUAP), we chose db6 for the mother wavelet. Also, in order to up-sample and inverse the filter coefficients without changing the meaning of the filter, the signal should be orthogonal. Daubechies wavelets are orthogonal [48]. Figure 9 shows as the level of the wavelet coefficient increase the resolution of the frequency decrease. The level one shows the rapid fluctuation of the signal at the expected delay, but in the level 4 we have poor frequency resolution.

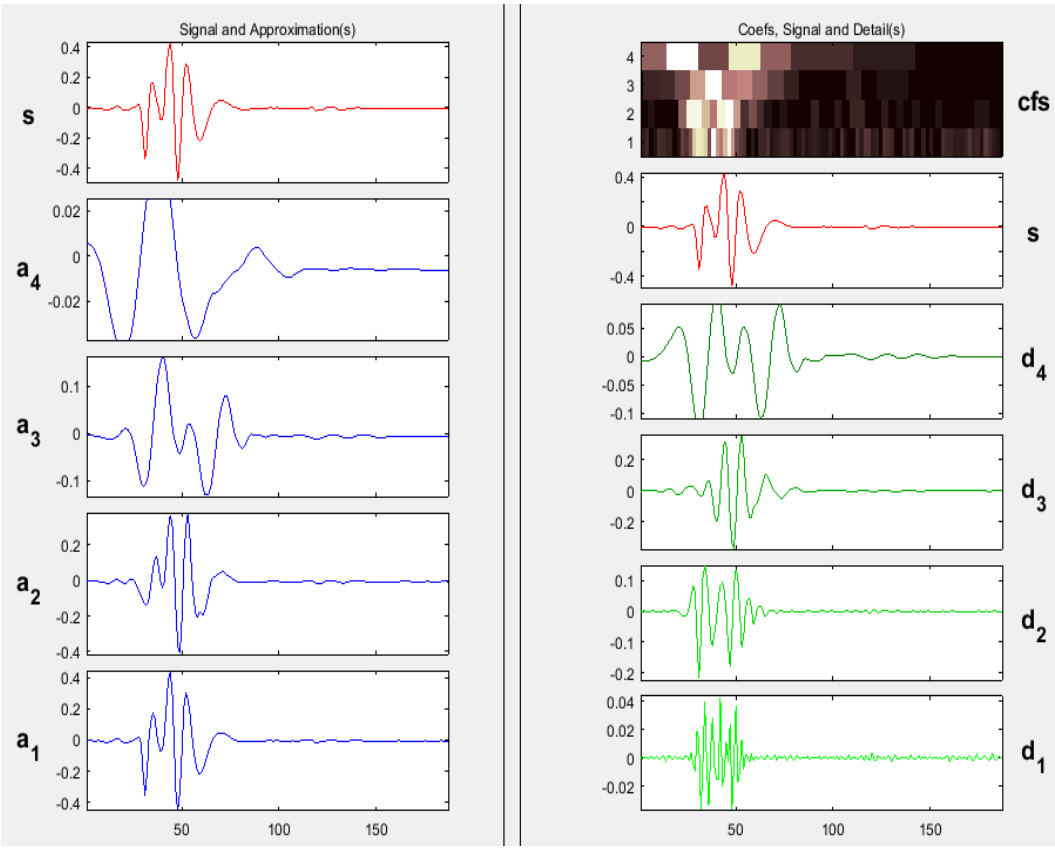

Figure 9. The four levels of the discrete wavelet coefficients of the response signals are shown as (a_1-a_4) approximations and (d_1-d_4) details. As the level increases the resolotion of the frequancy decreases.

3.6.1 Total energy of DWT coefficients. The total energy (area under the curve or energy) was calculated for first 3 approximations level of the wavelet coefficients as the contained the higher frequency component. The total energy of each level of the wavelet coefficient was obtained using an FFT-based power spectral density (PSD) analysis" pwelch" in Matlab. Then, the area under the curve of each level was calculated and this process repeated for all of the signals, i.e. in the left and right knee and ankle.

3.7 Time-Frequency Domain Analysis of Empirical Mode Decomposition

EMD, introduced by Huang et al. [49], is a signal processing technique based on local characteristics of the data in the time domain. The EMD method is based on the concept of instantaneous frequency defined as the derivative of the phase of an analytic signal. In EMD, the signal is decomposed into a finite number of intrinsic mode functions (IMFs). An IMF is defined as a function that satisfies two conditions: (1) the difference between the number of extrema (including both the local maxima and minima) and zero-crossings in the signal should not differ by one; (2) the mean value of the upper envelop (defined by maxima) and lower envelop (defined by minima) is zero through the entire signal. The sifting process is defined as a decomposition technique that sequentially extracts the IMFs from the original signal. First, the envelopes of the upper and lower side of the signal are determined. Second, the mean of the extremums is calculated. Third, the first component was found by differences between signal and the mean of extremums. If the first component satisfies the IMF condition and stopping criteria during the sifting process, it is considered as an IMF. The whole process is terminated when the residual component (the differences of the original signal and IMF) is either monotonic function or has more than one maximum. The flowchart of the EMD are shown in Figure 10.

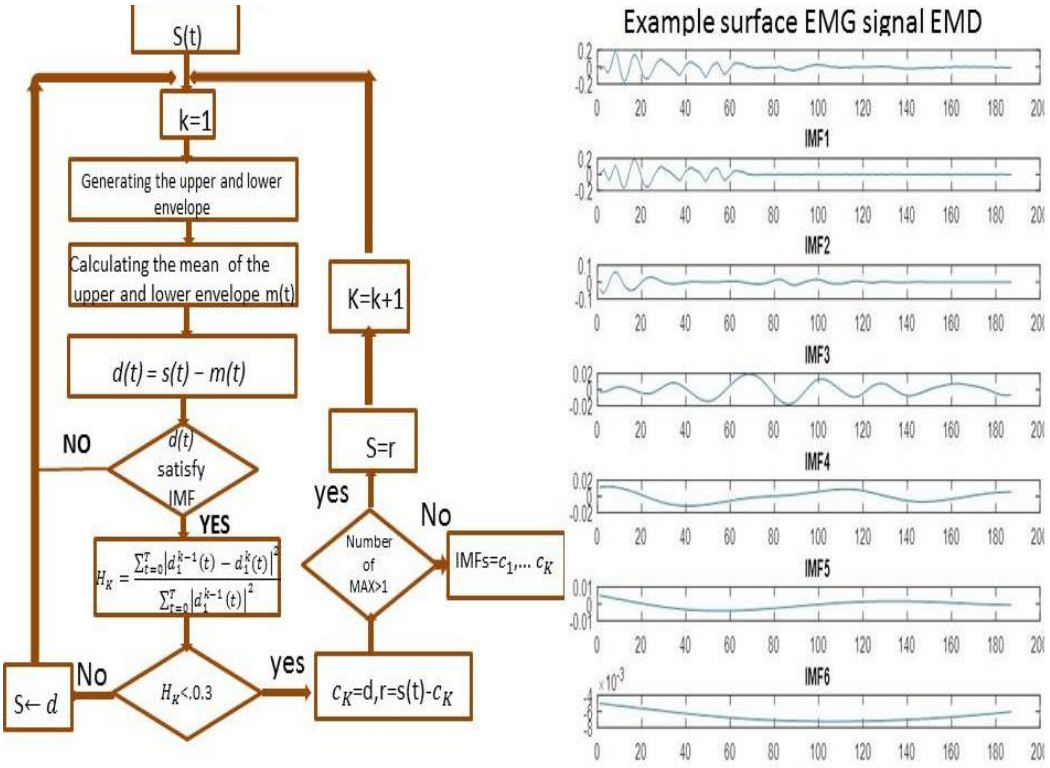

Figure 10. Flowchart is depicting the process of EMD. Six IMFs were extracted from the response signal.

3.7.1 Total energy of IMFs. The total power spectrum densities (i.e. total energy) of first and second IMFs were calculated. Hyperreflexia is characterized by higher amplitude in the time domain as well as higher oscillations in the frequency domain. Therefore, we considered the first and second IMFs, as they contain the higher frequency content.

3.7.2 Mean frequency of IMFs. The Mean frequencies (MNF) of the first and second IMF *of the response signal were calculated. The MNF has been widely used as a frequency-domain feature, especially when assessing muscle fatigue* [50]. Muscle fatigue is the reduction in the maximum tension generated by the patient, and may show up as a reduction of high frequency content in the signal, but not as amplitude changes

(Figure 8). To get the mean frequency of IMFs, first the IMFs were submitted to this process, which is defined as:

$$\hat{g}(t) = \frac{1}{\pi}\int_{-\infty}^{\infty} \frac{g(\tau)}{t-\tau}\, d\tau, \qquad (3\text{-}7)$$

where, $g(t)$ is the IMFs of the signal and $\hat{g}(t)$ is the Hilbert transform of the IMFs. The analytic signal is defined as:

$$z(t) = g(t) + i\hat{g}(t) = a(t)e^{i\theta t}, \qquad (3\text{-}8)$$

$$a(t) = \sqrt{g^2(t) + \hat{g}^2(t)}, \qquad (3\text{-}9)$$

$$\theta(t) = \arctan\left(\frac{\hat{g}(t)}{g(t)}\right), \qquad (3\text{-}10)$$

where $a(t)$is the amplitude of the analytic signal and $\theta(t)$ is the phase. The analytic signal is the best local fit to time series $g(t)$ in the form of a trigonometric function, which is amplitude and phase modulated. The instantaneous frequency of the Hilbert spectrum is defined as:

$$w(t) = \frac{d\theta}{dt}, \qquad (3\text{-}11)$$

Then the mean instantaneous frequency (MIF) of IMFs with m data points is defined as the weighed mean $\omega(t)$ using the square of $a(t)$ times the weight. It is defined as:

$$MIF = \frac{\sum_{i=1}^{m} w(i)a^2(i)}{\sum_{i=1}^{m} a^2(i)}, \qquad (3\text{-}12)$$

Figure 11and Figure 12 show that the instantaneous frequency decreases as the level of the IMFs increases. This is because the first level has the smallest time scale which corresponded to the fasted time variation of the signal.

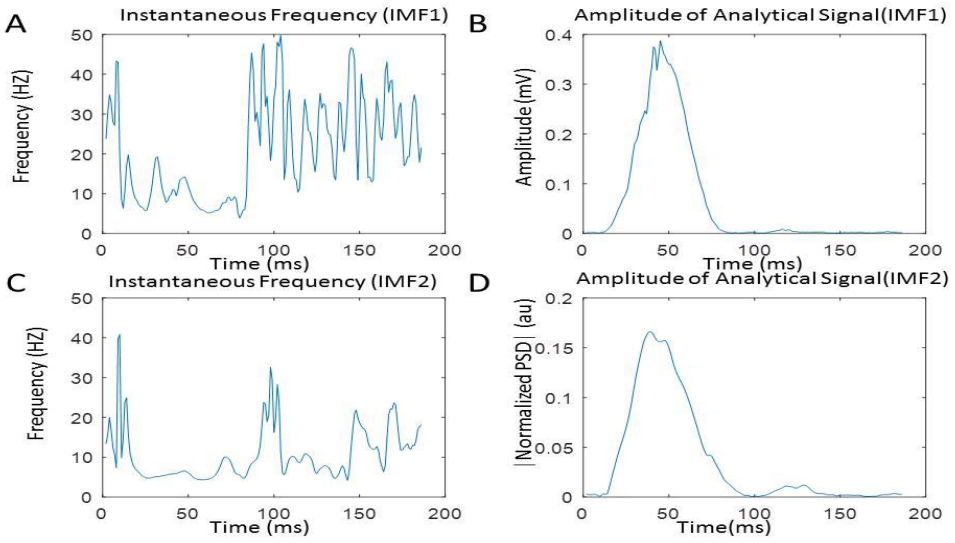

Figure 11. Instantaneous frequency of intrinsic mode functions (IMF1 and IMF2) as a function of time are shown in A and C. The amplitude of analytic signal of (IMF1 and IMF 2) as a function of time are shown in B and D.

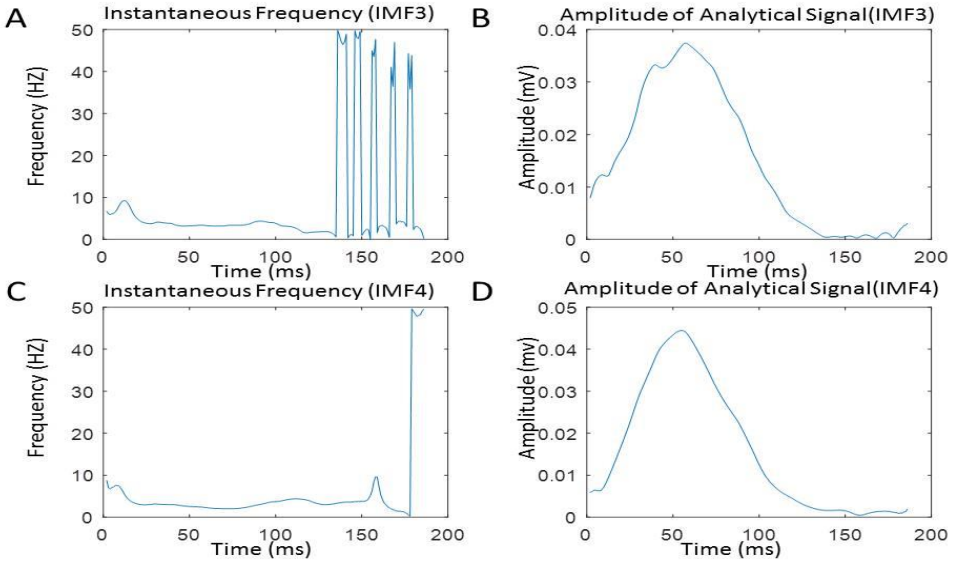

Figure 12. Instantaneous frequency of intrinsic mode functions (IMF3 and IMF4) as a function of time are shown in A and C. The amplitude of analytic signal of (IMF3 and IMF 4) as a function of time are shown in B and D.

Chapter 4

Statistical Analysis

4.1 Multivariate Linear Regression Model

Multivariate linear regression (MLR) of latency was defined as a linear function of every independent variable that influences latency (i.e. height, weight and age). The following multivariate linear regression model was used:

$$L \cong b + a_1(x_1 - \bar{x}_1) + a_2(x_2 - \bar{x}_2) + a_3(x_3 - \bar{x}_3), \quad (4.1)$$

where x_1 is age, x_2 is weight and x_3 is height; $\bar{x}$ denotes the average of quantity x; L is the nonnormalized and b the normalized latencies. By applying multi-linear regression, the coefficients of the regression for each group were calculated. When these coefficients are property normalized, they show the strength of each independent variable (age, weight and height) on the latency, in both the knee and ankle reflexes. These coefficients were used to normalize latency for each patient, so as to remove any effects based on physical characteristics, which may vary between the groups. A paired T-test between the nonnormalized and normalized latencies was performed to determine if there was a significant effect of normalization.

4.2 Tests for Normality

Before applying any statistical analysis, it must be ascertained if the data fit a normal distribution. The result determines which kind of statistical test can be used to analyze the data set. *One sample Kolmogorov Smirnov* test was performed to determine the normality of the data set by comparing the random sample from the data set with a normal distribution of that random variable. One logical way of comparison is taking the mean of the empirical distribution function which is defined as follow:

$$S(x) = \frac{1}{n}\sum_{i=1}^{n} I\{x_i \leq x\}, \qquad (4.2)$$

where $S(x)$ is empirical distribution function, n is the number of samples and x is the samples. *Kolmogorov* compares the hypothesized distribution function with empirical distribution function by measuring the largest distance between two functions:

$$T = |S(x) - F(x)|, \qquad (4.3)$$

where $F(x)$ is the hypothesized distribution. In order to reject the null hypothesis (data come from a normal distribution) at level of significance, T must be bigger than $1 - \alpha$ as given by the table in [51].

4.3 The Analysis of Variance: One -Way ANOVA

ANOVA is usually used for analyzing the differences such as mean and variance within and between groups for more than two populations. The factors are the characteristics that differentiate the populations in different groups from one another, i.e. latency is one factor in the experiment among 7 groups of populations. The between-samples variation and within sample variation can be shown as mean square for treatment (MSTr) and mean square error (MSE), respectively[52].

$$MSTr = \frac{1}{I-1}[(\bar{x}_{1.} - \bar{x}_{..})^2 + \cdots + (\bar{x}_{I.} - \bar{x}_{..})^2] = \frac{1}{I-1}\sum_{i=1}^{I}(\bar{x}_{i.} - \bar{x}_{..})^2, \qquad (4.4)$$

J= sample size of each population.

$$S_i^2 = \frac{\sum_{j=1}^{j}(x_{ij} - \bar{x}_{.})^2}{J-1} \quad i = 1, \ldots, I, \qquad (4.5)$$

$$MSE = \frac{S_1^2 + S_2^2 + \cdots + S_I^2}{I}, \qquad (4.6)$$

$$F = \frac{MSTr}{MSE}, \qquad (4.7)$$

If null hypothesis H0 (all the groups have the same variance) is true, F will have an F distribution with $v_1 = I - 1\ , v_2 = I(J-1)$. The rejection region is $f > F_{\alpha,I-1,I(J-1)}$ for the significant level of α.

4.4 The Kruskal-Wallis Test (KW)

The Kruskal-Wallis test is non-parametric test and therefore is not dependent on any assumption of a particular distribution. KW test is based on observing the rankings of the observations, and comparing them to rankings that would be expected under the null hypothesis.

Let x_{ij} be j^{th} observation from i^{th} sample and r_{ij} be the rank of them. Let $\bar{r}_{I.}$ be the average of all ranks. If H_0 is true, then:

$$\boldsymbol{E}(r_{ij}) = \frac{N+1}{2} \qquad E(\bar{r}_{I.}) = \frac{1}{j_i}\sum_j r_{ij} = \frac{N+1}{2}, \qquad (4.8)$$

The deviation of each rank from the common expected value is measured by KW test. H_0 is rejected if there is too much deviation from the expected value. This statistic is:

$$K = \frac{12}{N(N+1)}\sum_{i=1}^{I} j_i\,(\bar{r}_{I.} - \frac{N+1}{2})^2, \quad (4.9)$$

K must be big enough to reject the null hypothesis, i.e. $K \geq C$. Where C is obtained for desired α as provided in [53].

4.5 Two Sample T-Test

For a two-sample *t*-test, the null hypothesis is that the mean vectors x and y both from the normal distribution are equal but the variances are unknown. When data in x and y come from populations with different means, then the null hypothesis is rejected. The test statistic is defined as: [54]

$$t = \frac{\bar{x} - \bar{y}}{\sqrt{\frac{\overline{s_x^2}}{n} + \frac{\overline{s_y^2}}{m}}}, \qquad (4.10)$$

where $\bar{x}$ and $\bar{y}$ are the sample means, s_x and s_y are the sample standard deviations, and n and m are the sample sizes. The two-sample *t*-test was used to compare the left to the right of the knee and ankle features.

Chapter 5

Results

Deep tendon reflexes of the knee and ankle were recorded prospectively in 279 healthy subjects aged 15-48 years old in this study (table 1). 21 women in the first trimester (defined as gestational age 1-14 weeks and 6 days), 48 in the 2nd trimester (15-27 weeks and 6 days), 42 in the 3rd trimester (28-36 weeks and 6 days), 25 at term (37 to 42 weeks), 51 at day 1 or 3 postpartum, 47 non pregnant women, and 45 men. The demographic characteristics of data are provided in Table 1. There were some significant differences between the groups. The men were significantly taller than the women in all other groups (177 ± 8.8cm vs 161.3 ± 7.5cm; $p < 0.001$). Despite being heavier (83.6kg vs 76.7kg), men had a lower BMI than women in 3rd trimester and term (26.7 ± 5.3kgm^{-2} vs 30.0 ± 6.1kgm^{-2} and 31.1 ± 7.3kgm^{-2}; $p = 0.006$). The weight of men showed greatest difference with the non-pregnant women and 2nd trimester of pregnancy (83.6 ± 17.0kg) ves 74.4±19.0kg and 74.0±19.0kg; $p = 0.004$). The mean ages were similar for all the groups ($p = 0.18$).

5.1 Latency Definition: Peak to First Peak

Latency was defined in 3 different ways as shown in Figure 3A-C, from peak of impulse (reflex hammer strike) to onset of reflex response envelope (peak-to-onset; Figure 3A), from peak of impulse to the first peak of response signal (peak-to-first peak; Figure 3B), or from peak of impulse to highest peak of response signal (peak-to-peak; Figure 3C). The number of outliers and standard deviation of latency by the 3 definitions, in each of the 7 groups is shown in Figure 13. These values were obtained from the 30-tap trials from each knee and ankle for all patients. The peak-to-first peak

definition was most robust with the lowest number of outliers (101 versus 110 for peak-to-peak and 117 for peak-to-onset) as well as smallest standard deviation (4.3 compared to 4.8 for peak-to-onset and 6.3 for peak-to-peak). Therefore, peak-to-onset had the highest number of outliers and peak-to-onset had highest standard deviation. We therefore adopted peak-to-first-peak definition of the DTR latency for further analysis.

Table 1

Participant Characteristics, by Group (N = 279 Healthy Volunteers)

	Age (years)	Height (cm)	Weight (kg)	BMI (Kg/m^2)
Men (n=45)	26.8±6.7 (19-48)	177.0±8.8 (157-203)	83.6±17.0 (59-113)	26.7±5.3 (19.8-46.0)
Non-pregnant (n=47)	28.0±8.6 (17-48)	162.7±6.0 (149-177)	74.4±19.0 (47-118)	28.1±6.9 (18.7-43.4)
1-14.6 weeks Pregnant (n=21)	24.3±6.0 (18-40)	163.3±7.6 (144-177)	76.9±19.7 (49-110)	28.9±7.5 (19.2-46.0)
15-27.6 weeks Pregnant (n=48)	24.6±4.7 (17-35)	159.3±8.1 (147-152)	74.0±19.0 (52-152)	29.0±7.5 (20.6-51.2)
28-36.6 weeks Pregnant (n=42)	25.8±5.4 (18-38)	161.4±6.5 (142-180)	79.0±19.5 (50-153)	30.0±6.1 (19-53)
37-42 weeks Pregnant (n=25)	25.9±6.5 (15-39)	161.6±8.1 (144-177)	80.9±19.0 (52-123)	31.1±7.3 (21.4-46.2)
Postpartum (n=51)	25.9±5.6 (17-39)	162.2±10.8 (142-175)	75.9±19.0 (47-122)	28.9±7.1 (18.2-44.9)
p-value	0.18^{K}	$8.0E\text{-}35^{A}$*	0.004^{K}*	0.006^{K}*

Note. n = number of participants in each group. Pregnancy gestational ages are denoted using the format weeks.days, e.g. 14.6 = 14 weeks and 6 days. The range of each group characteristic is presented in parenthesis. ^{K} = p-value obtained with one-way Kruskal-Wallis test. A = p-value obtained with one-way ANOVA test. Each value is denoted as mean ± sd. * = significant difference (i.e. $p < 0.05$).

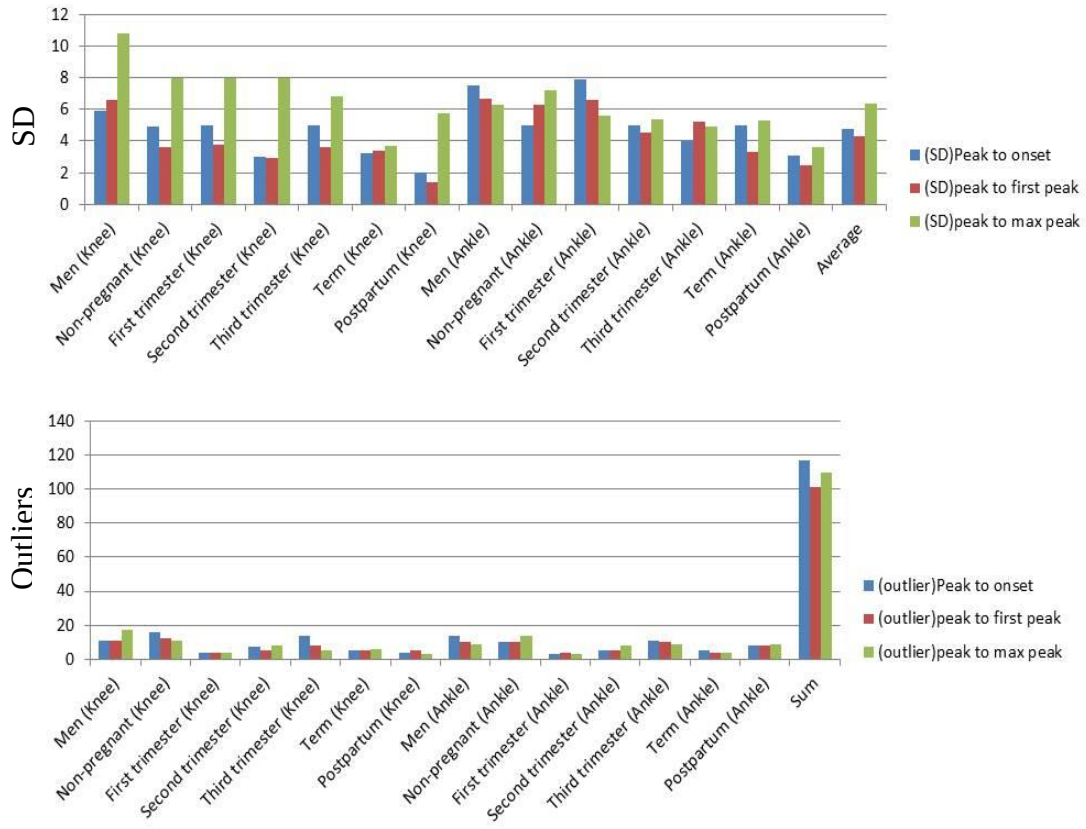

Figure 13. Effect of latency definition. Latency standard deviation (SD) and number of outliers as a function of latency definition in knee and the ankle.

5.2 Comparison of the Right and Left Sides

When the latency values for right and left knee reflexes were compared by paired-sample t-test, the outcome measurements showed no significant difference between the left and right knee in each of the 7 groups, as shown in Table 2. Similar findings were seen for the ankle reflex latency. Therefore, the signals of the 2 sides were combined resulting in ~60 reflex taps per site (knee and ankle) per patient. There was data from 16,740 knee signals and similar number of ankle signals analyzed.

Table 2

Paired Sample T-Test for Left and Right Knee

Knee	Men	Non pregnant	First stage	Second stage	Third stage	Term	Post-partum
h	0	0	0	0	0	0	0
p	0.22	0.40	0.87	0.11	0.93	0.22	0.56
Ankle	Men	Non pregnant	First stage	Second stage	Third stage	Term	Post-partum
h	0	0	0	0	0	0	0
p	0.06	0.57	0.24	0.57	0.39	0.84	0.65

Note. h: Test decision for the null hypothesis that the data comes from independent populations with equal means. The result h is 1 if the test rejects the null hypothesis at the 5% significance level, and 0 otherwise, P = p-value.

5.3 Mean versus Mode of Latency and Effect of Number of Trials

In order to determine how many trials are needed to obtain a stable latency value in the knee and ankle, the latency was averaged as a function of the number of the trials using both the latency mode and mean for each subject in groups 1 and 2 (166 observations for knee and 155 observations for ankle). As the number of trials increase, the mode converges quickly, while the mean sometimes converges. Figure 14shows an example of this finding in 4 males and 4 non-pregnant female subjects. The mode of latencies performed better and converged faster compared with the mean for the large sample of trials (arrow in Fig 14 denotes convergence). The mode was also more stable, while the mean had more variability. These data also show that there is no reflex decay with increasing number of trials as suggested by some investigators [20, 43].

A stable mode of latency (the point that adding more trials doesn't change the latency) for the knee reflex was obtained after 5 trials in almost half of the subjects

(Figure 15). However, 15 trials were needed to obtain the stable value in >85% of the population, and was similar in both ankle and knee.

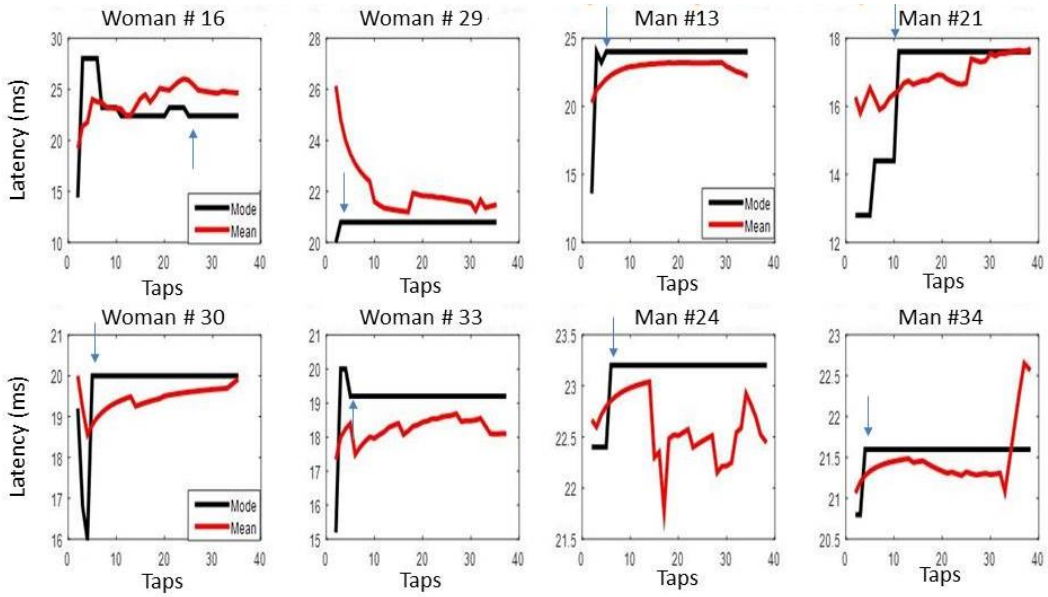

Figure 14. Latency as a function of the number of the trials using mode and mean calculations is shown in the black and red lines, respectively for 4 healthy men and 4 healthy women.

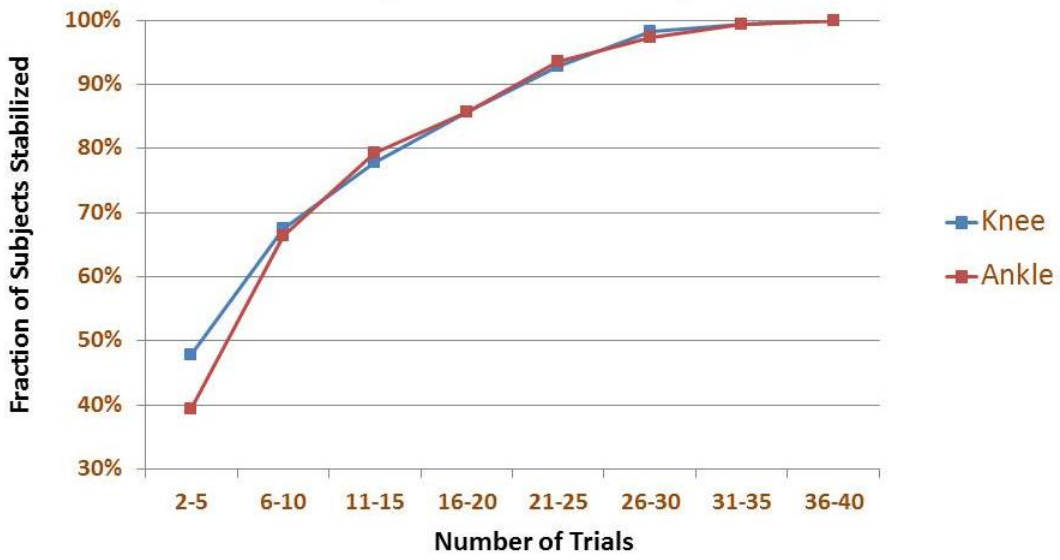

Figure 15. The cumulative stabilization of the latency as a function of the number of trials shows the percentages of data that reach to the stabilized latency (the point that adding more trials doesn't change the latency) from 166 knee taps and 155 ankle taps (left and right combined) of non-pregnant female and male participants.

5.4 Normalization of the Latency Based on Age, Height and Weight

The latencies of the groups were plotted as a function of age, height and weight to look for effects (Figure 16). There is a slight increase in the latency with the age and possible effects of weight, height or BMI. To correct for possible differences of age, height and weight of subjects between the groups on the group latency as well as to isolate each of these effects, multiple linear regression was performed. The coefficients of the regression for age (a_1), weight (a_2) and height (a_3) were calculated as (0.0065, -0.015, 0.019) for the knee and (0.0053, 0.0027, 0.014) for the ankle. These coefficients show the strength of each independent variable (age, weight and height) on the latency, in both the knee and ankle reflexes. However, the regression coefficients have different units. In order to compare their effect strength, we normalized them to the average factor (table 3). Height has the greatest effect on the latency compared with the other parameters, in both the knee and ankle reflexes when all groups are combined. These coefficients were then used to normalize latency for each patient.

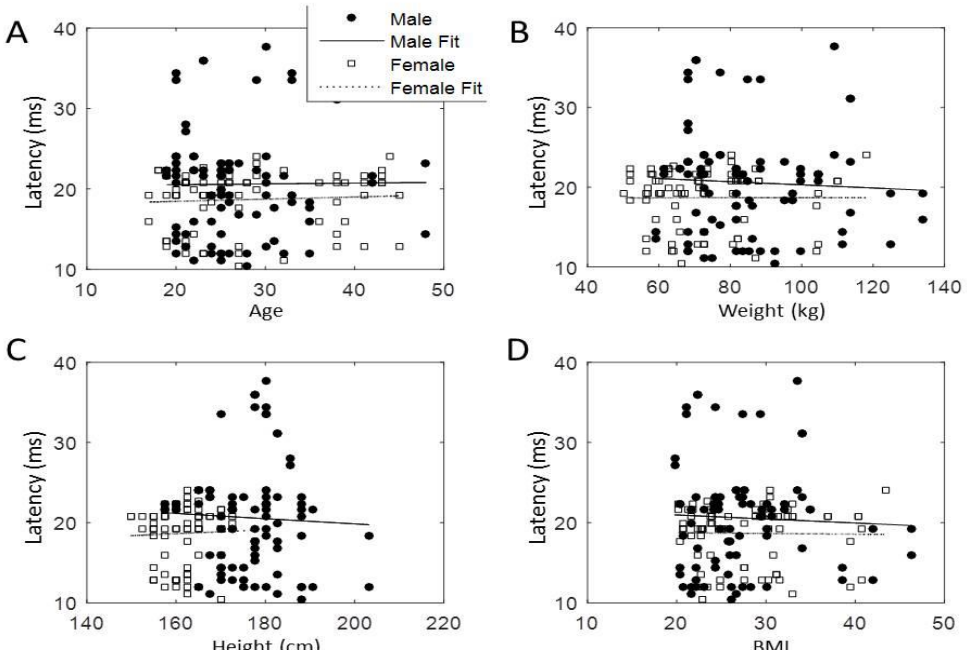

Figure 16. The dependence of the latency on subject characteristic as a function of (a) age, (b) weight, (c) height and (d) body mass index (BMI). Data is shown for all males as well as non-pregnant females in the knee.

Table 3

The Multiple Linear Regression Coefficients for Combined Men and Women

	Knee			**Ankle**		
Coefficient	$\boldsymbol{a_1}$ (age)	$\boldsymbol{a_2}$ (weight)	$\boldsymbol{a_3}$ (height)	$\boldsymbol{a_1}$ (age)	$\boldsymbol{a_2}$ (weight)	$\boldsymbol{a_3}$ (height)
Raw coefficient	0.006 ms/yr	-0.01 ms/kg	0.02 ms/cm	0.005	0.003	0.02
Average factor	26 yr	77 kg	164 cm	26	77	164
Normalized Coefficient (ms)	0.17	-0.77	3.28	0.13	0.23	3.28

5.5 Latency and Sexual Dimorphism

The latency of the knee and ankle reflex in men are ~2ms longer than in non-pregnant women. To determine if the tallness of men (177 ± 8.8cm versus 162.7 ± 6.0cm) was contributing to the delay in latency in men, the latencies were plotted as a function of height before and after combining the male and female groups (Figure 17). In the knee, male latency slightly decreased with height while female slightly increased (fig 17a); there was no apparent effect in the ankle (fig 17c). The slopes of the lines are -0.032ms/cm, -0.022ms/cm for male knee and ankle reflex, respectively; and 0.024ms/cm, 0.0052ms/cm for female knee and ankle reflex respectively. When the combined latency from both men and women is plotted as a function of height (Figures 17B-C), the slope of the curve is greater in both the knee and the ankle (0.057ms/cm, 0.067ms/cm, respectively) suggesting a false impression of height effect when data are combined and there is smaller and no consistent effect individually on the groups over a large height range. Thus latency delay in men is not due to their height and is due to sexual dimorphism (i.e. a difference between the sexes). Therefore, the multiple linear regression analysis was revised and the sexual dimorphism was taken into account by fitting the groups independently. The results after revision (table 4) shows that the height and weight coefficients are inconsistent in the knee and in the ankle therefore they are of uncertain significance. The age coefficient is positive for both groups and at both locations (in the knee and the ankle) and the effect on latency is 1.7x in ankle (1.95) compared to the knee (1.15). This suggests that there is a reduction in conduction velocity as a function of age, leading to the observed increased latency, which increases as a function of distance traveled.

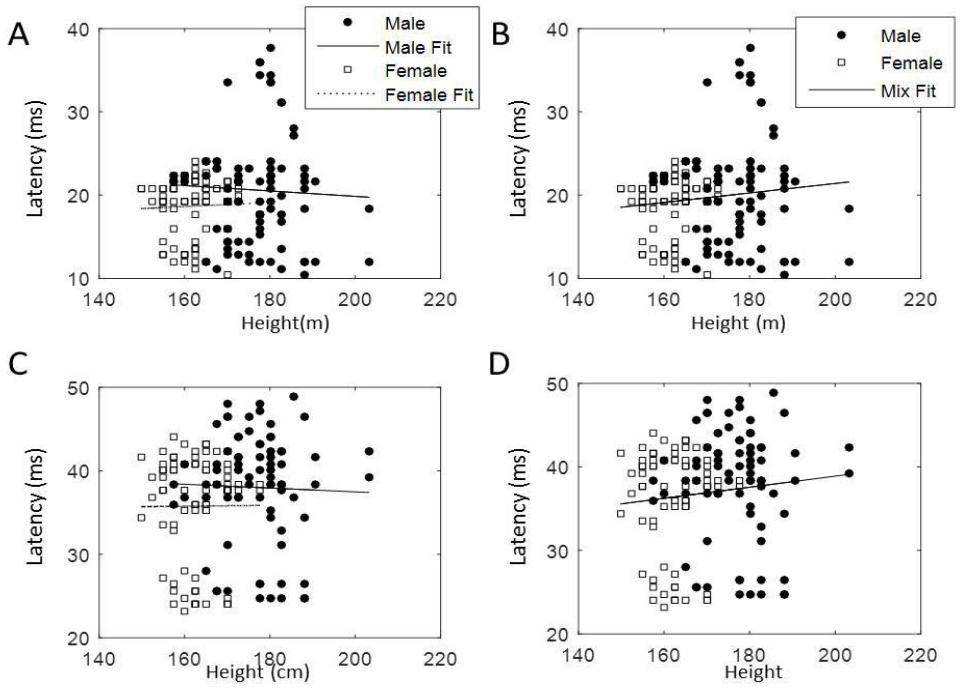

Figure 17. The dependence of latency as function of height is shown for both combined and noncombined data. Uncombined sexes (A) and combined sexes (B) in the knee; Uncombined sexes (C) and combined sexes (D) in the ankle.

Table 4

Revised Multiple Linear Regression Coefficients for Men and Non-Pregnant Women Fitted Separately

	a_1 (ms/ year)	Average regressor (year)	$\tilde{a}_1$ ms	a_2 (ms/ kg)	Average regressor (kg)	$\tilde{a}_2$ (ms)	a_3 (ms/ cm)	Average regressor (cm)	$\tilde{a}_3$ ms
Men knee	0.05	27	1.3	-0.04	85	-3.3	-0.03	176	-5.6
Non-pregnant knee	0.03	28	1.0	0.03	72	2.2	0.02	162	3.8
Men Ankle	0.10	26	2.6	.051	81	4.1	-0.02	174	-3.8
Non-pregnant Ankle	0.05	28	1.3	-.024	73	-1.7	.005	162	0.8

Note. ã is the normalized coefficient.

5.6 Latency and the Phases of Pregnancy

The latency of the ankle reflex (35.8 ± 6.4ms) was almost twice that of the knee reflex (18.7 ± 6.6ms), as expected due to farther distance travelled by the signal from the muscle to the spinal cord and back. The latency of the knee reflex was 1.9ms longer in males (20.6ms, ci= [19.1-22.4]) compared to non-pregnant females (18.7ms, ci= [17.9-19.5]) a difference that is highly statistically significant ($p < 0.001$). Similarly, the latency for the ankle reflex was also 2.2ms longer in males (38.0ms, ci= [36.4-39.5] versus 35.8ms, ci= [34.3-37.2], respectively). The mean latency and confidence intervals for the mean of the 7 groups are presented in Table 5. For all group-wise statistical analyses, the non-pregnant female group was designated as the reference unless there was a statistically significant difference with respect to another group (e.g. knee duration analysis). In pregnancy, the latency in both the knee and ankle reflexes was statistically unchanged before 15 weeks' gestation (i.e. first trimester), but there is a trend towards prolongation with increasing gestational age (Table 5 and Figure 18A&B). The latency delay reached statistical significance in both the term and postpartum period in the knee and post-partum only in the ankle. Figure 18shows the box and whisker plots of knee and ankle latencies for the seven groups before and after normalization. The normalization changed the group standard deviations a bit as well as altering some of the outliers, however, it did not alter the result trends or group-wise significance of the results. There was no statistically significant difference between normalized and non-normalized latency using paired t-test ($p=1.0$ for both knee and ankle). The normalization may be more important for comparing a specific patient to the mean in subsequent analysis.

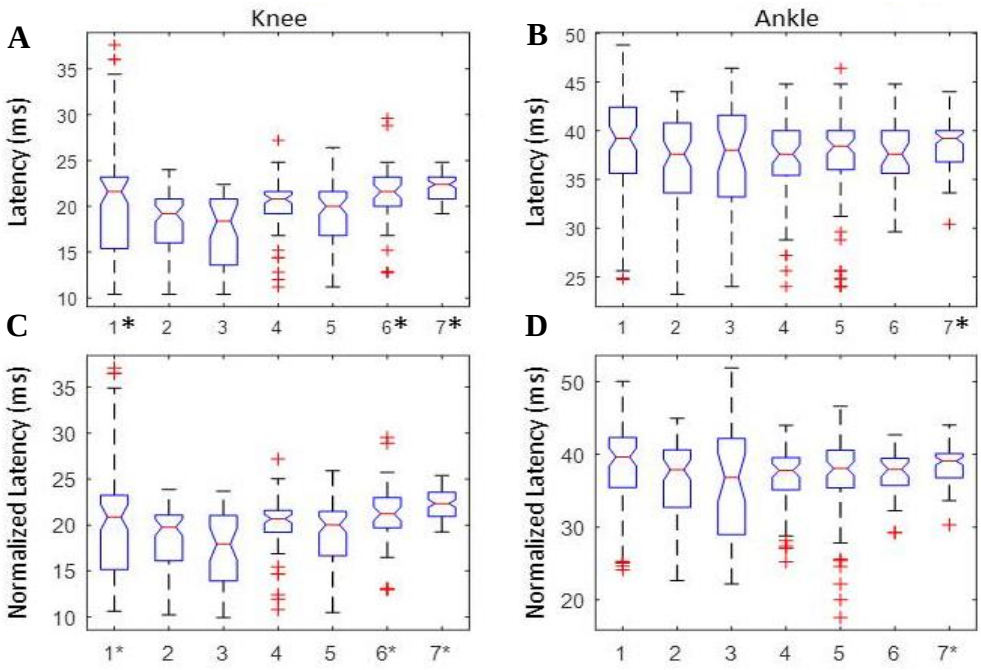

Figure 18. Group-wise latency as a function of pregnancy phase results of the using box and whisker plots. Latency in the (a) knee and (b) ankle as well as normalized latency in the (c) knee and (d) ankle. Group designations are: 1- males, 2- non-pregnant females, 3-first trimester, 4-second trimester, 5-third trimester, 6-term and 7-post-partum. * denotes significant deference with respect to the non-pregnant female group; (+) denotes outlier data.

5.7 Central Inhibition of DTR Latency

Using the latency in non-pregnant women as the baseline, the change in the latency in the different trimesters of pregnancy in both knee and ankle reflex are shown in Figure 19. A gradual increase in the latency with increasing gestational age is again seen. For the knee reflex, the difference of the latency with non-pregnant state is -1.2ms in the 1st trimester, 1.4ms in the 2nd trimester, 0.4ms in the 3rd trimester, 2.4ms at term, and 3.6ms in the postpartum period; the average increase in latency is 1.8ms in all trimesters. The corresponding values for the ankle reflex are -0.7ms, 1.4ms, 1.7ms, 3ms and 1.6ms, respectively. It is important to note that the average increases in the latency as a function of all stages of pregnancy at the knee and ankle is similar (all stages in

Figure 19). This suggests that the increase in latency in pregnancy is not a function of the distance travelled (otherwise the change in ankle latency would be double that of the knee latency). Therefore, this probably represents a central inhibition of the reflex arc at the level of the anterior horn synapse in the spinal cord as opposed to a change in conduction velocity of the nerve (which would have prolonged the ankle reflex more than the knee reflex). Therefore, the delay is likely explained by central inhibition of the reflex at the spinal cord rather than being explained by a change in conduction velocity (for example caused by perineural edema) in pregnancy. We hypothesize that the gradual increase in latency throughout pregnancy is an inhibitory CNS effect gradually increasing over the course of pregnancy.

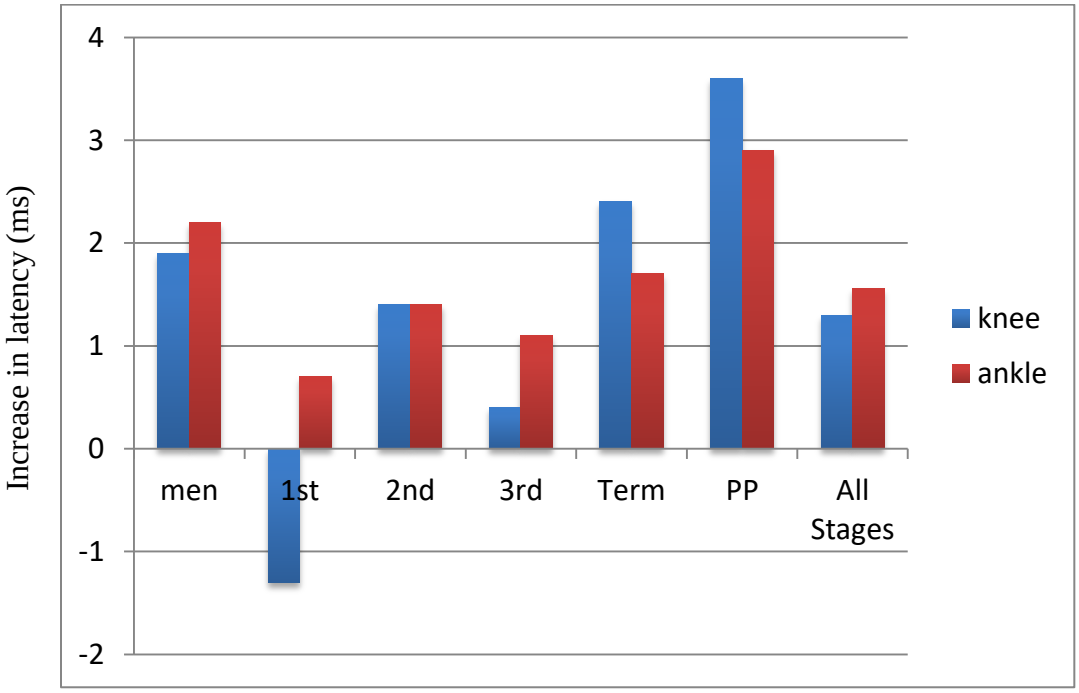

Figure 19. Average latency difference of all groups from the non-pregnant females. The last column represents the average difference of all stages of pregnancy compared to non-pregnant females. Note that the average latency difference throughout pregnancy is similar in the knee and ankle.

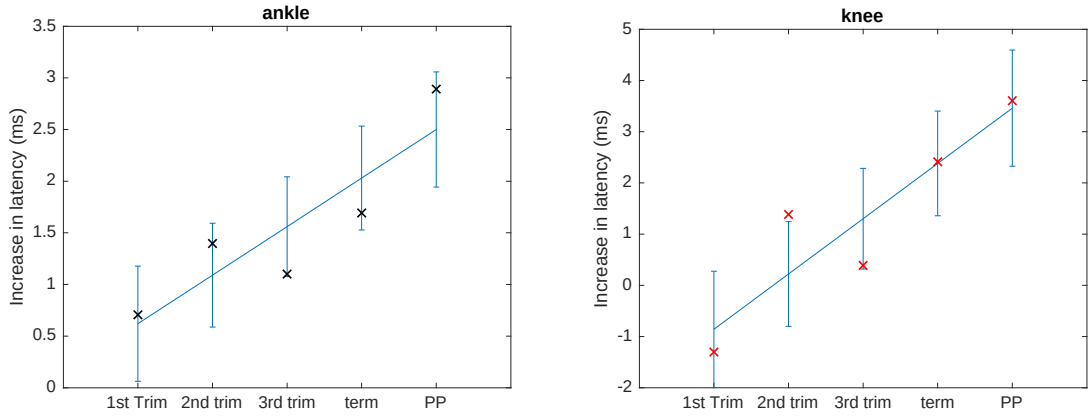

Figure 20. Change in latency during pregnancy fitted to a line. X denotes the data points and the line is the linear fit. Note the increase in latency during pregnancy. The error bars represent standard deviation at each observation point.

5.8 Amplitude Results

The average of the amplitude in the ankle reflex is approximately 4 times that of the knee (1.3 ± 1.1mv vs. 0.3 ± 0.22mv, p-value = 1E-83). There is a larger variability in the amplitude of the reflex noted (large SDs compared to the mean shown in Table 5), a known limitation of amplitude analysis. There was no significant difference between the groups in the ankle. In the knee, there were significant increases in reflex amplitude in the second trimester and post-partum with respect to non-pregnant females (0.41±0.29mv and 0.46±0.24mv vs. 0.26±0.18; p<<0.001 (Table 5), of unknown clinical significance.

5.9 Duration Results

The duration of the DTR response signal is similar in the knee and ankle (~50ms). There were no significant differences in the mean duration of the knee or ankle reflex in any of the groups, when compared to the non-pregnant female subjects (Table 5 and Figure 21A&B). There was a significant increase in duration between post-partum females and 3rd trimester in the knee only, of doubtful clinical significance.

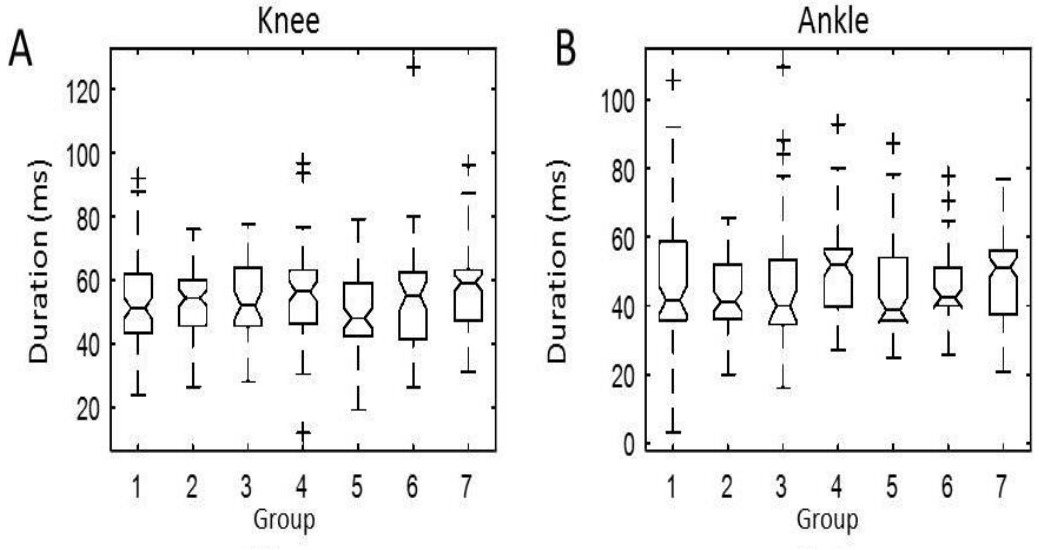

Figure 21. Duration results in the knee (a) and ankle (b) of the response signal for all groups. The group designations are the same as prior figures.

Table 5

Subjects' Time-Domain Features and Their Confidence Intervals, By Group

	Latency Knee (ms) [CI]	Latency Knee (ms) Normalized	Latency Ankle (ms)	Latency Ankle (ms) Normalized
Men	20.6 ± 6.6* [19.15,22.4]	20.6 ± 6.6* [19.1,22.0]	38.0 ± 6.7 [36.4,39.5]	38.0 ± 6.7 [36.4,39.5]
Non-pregnant	18.7 ± 3.6† [17.9,19.5]	18.7±3.6† [17.9,19.5]	35.8 ± 6.4† [34.3,37.2]	35.8 ± 6.5† [34.2,37.2]
1st Trimester	17.4 ± 3.8 [16.2,18.6]	17.4±3.8 [16.2,18.6]	36.5 ± 6.7 [34.4,38.6]	36.5 ± 8.2 [33.8,39.1]
2nd Trimester	20.1 ± 2.9 [19.4,20.8]	20.1±2.9 [19.4,20.8]	37.2 ± 4.4 [36.0,38.4]	37.2 ± 4.2 [36.1,38.3]
3rd Trimester	19.1 ± 3.6 [18.2,19.9]	19.1±3.5 [18.2,19.8]	36.9 ± 5.2 [35.7,38.2]	36.9 ± 5.8 [35.6,38.3]
Term	21.1 ± 3.5* [20.1,22.2]	21.1±3.4* [20.1,22.1]	37.5 ± 3.3 [36.5,38.6]	37.5 ± 3.1 [36.4,38.5]
Postpartum	22.3 ± 1.4* [22.0,22.6]	22.3±1.4* [22.0,22.6]	38.7 ± 2.5* [38.2,39.3]	38.7 ± 2.5* [38.2,39.3]
ANOVA P-value	7E-12	6E-12	0.02	0.03

Table 5 (Continued)

	Duration Knee (ms)	Duration Ankle (ms)	Amplitude Knee (mv)	Amplitude Ankle (mv)
Men	52.8 ± 13.6 [49.9,55.9]	46.9 ± 18.2 [42.8,51.0]	0.23 ± 0.2 [0.18,0.27]	1.3 ± 1.0 [1.1,1.6]
Non-pregnant	53.1 ± 9.2 [51.1,55.6]	43.6 ± 10.1 [41.4, 45.8]	0.26 ± 0.18† [0.22,0.30]	1.5 ± 1.1 [1.3,1.8]
1st Trimester	54.3 ± 11.7 [50.5,58.0]	44.6 ± 20.6 [37.9, 51.3]	0.24 ± 0.22 [0.17,0.31]	1.1 ± 1.2 [0.7,1.5]
2nd Trimester	54.6 ± 13.7 [51.4,57.8]	49.4 ± 12.2 [46.4,52.5]	0.41 ± 0.3* [0.34,0.47]	1.6 ± 1.3 [1.3,1.9]
3rd Trimester	50.4 ± 13† [47.4,53.4]	44.5 ± 13.1 [41.4,47.6]	0.17 ± 0.1 [0.14,0.21]	1.1 ± 1.0 [0.9,1.4]
Term	54.0 ± 17.3 [48.8,59.1]	45.8 ± 10.1 [42.7,48.9]	0.35 ± 0.32 [0.26,0.44]	1.2 ± 0.8 [0.9,1.5]
Postpartum	58.3 ± 12* [55.8,60.7]	48.6 ± 10.8 [46.4,50.7]	0.46 ± 0.2* [0.42,0.52]	1.3 ± 1.0 [1.1,1.5]
ANOVA P-value	0.01	0.08	9E-20	0.09

Note. p-value obtained with one-way ANOVA test, value reported as mean±sd, *=significant difference, ms = millisecond, mv = millivolt. †Denotes which group served as the baseline for comparison

5.10 Frequency Domain: Bandwidth

There was a gradual increase in the bandwidth of the DTR signal with advancing gestational age of pregnancy (Figure 22A & B). The increase in bandwidth was statistically significant in the post-partum period in the knee (mean=62.5Hz, ci= [57.4-67.5]) and ankle (mean=63.9Hz, ci= [61.8-66.3]) compared to the non-pregnant women (Table 6). The bandwidth in the ankle is higher than the knee (is this statistically significant?). Men and women's bandwidth is similar.

5.11 Frequency Domain: Mean Frequency

Mean frequency appears greater in the knee than the ankle. The mean frequency in the knee decreased with the stage of pregnancy and became significant in postpartum period (17.8 ± 6.4Hz) compared with the non-pregnant state (25.2 ± 10.2Hz) (Figure 22C &D as well as table 6). There was no statistically significant change in the mean frequency during pregnancy at the ankle.

5.12 Frequency Domain: Total Energy

The total energy of the response signal (area under the curve of Figure 3D) are presented in Table 6 and Figure 22E&F for both knee and ankle. There are large variations in response signal energy manifestoed as large standard deviations as well as large number of outliers. In the knee, total energy increased during pregnancy and became significant at term and post-partum versus the non-pregnant state (0.007 ± 0.01auHZ compared to 0.002 ± 0.003auHZ. No differences between groups were seen in the total energy of the response signal for the ankle reflex.

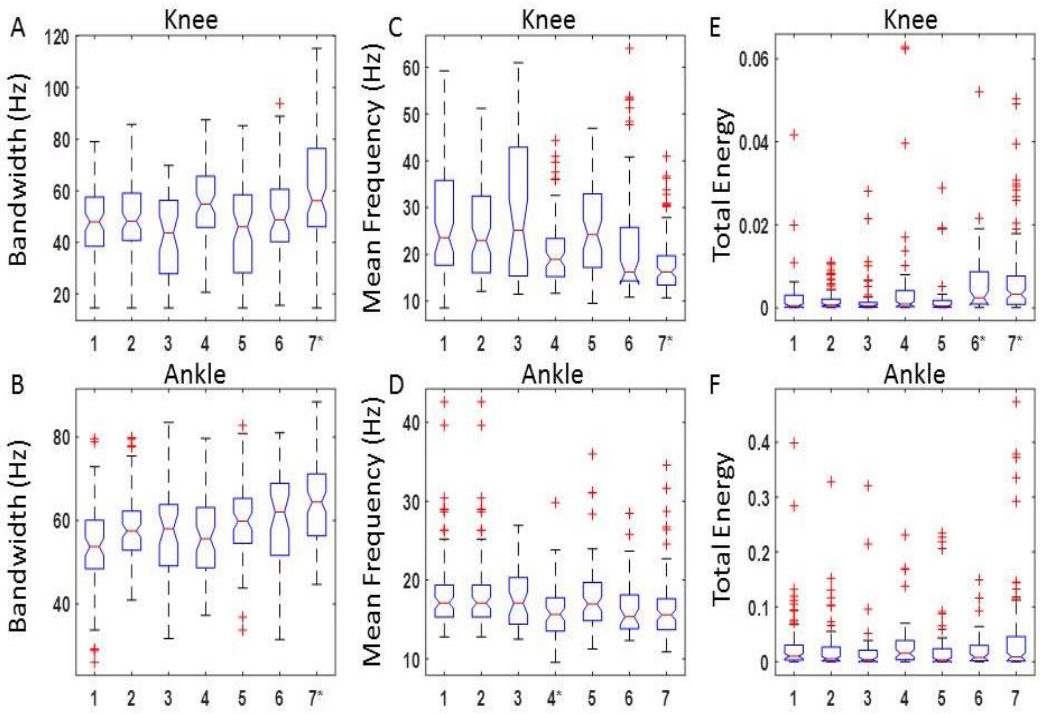

Figure 22. The bandwidth, mean frequency and total energy results of the response signal for various groups. Signal bandwidth in the (A) knee and (B) ankle. Mean frequency in the knee(C) and ankle (D). Total energy in the knee (E) and ankle (F). Group designations are: 1- males, 2- non-pregnant females, 3-first trimester, 4-second trimester, 5-third trimester, 6-term and 7- post-partum.

Table 6

Subjects' Frequency Domain Features and Their Confidence Intervals, by Group

	Bandwidth knee(Hz) (CI)	Bandwidth Ankle(Hz) (CI)	MNF knee(Hz) (CI)	MNF Ankle(Hz) (CI)	Total PSD Knee(mv) (CI)	Total PSD Ankle(mv) (CI)
Men	45.9±16.8 [42.2,49.6]	53.9±10.2 [51.5,56.3]	28.4±13.5 [24.4,31.4]	18.5±5.3 [17.2,19.7]	0.002±0.005 [0.001,0.003]	0.03±0.06 [0.017,0.044]
Non-pregnant	48.5±15.2† [45.2,51.7]	58.2±8.4 [56.3,60.0]	25.2±10.2† [23.0,27.4]	17.5±5.4 [16.4,18.7]	.002±0.003† [0.001,0.002]	0.02± 0.04 [0.013,0.032]
1st Trimester	42.2±17.1 [36.9,47.6]	57.7±11 [54.2,61.2]	29.2±15.2 [25.1,34.7]	17.6±3.6 [16.4,18.8]	0.003±0.004 [0.001,0.004]	0.02±0.06 [0.005,0.041]
2nd Trimester	55.4±14.7 [51.9,58.9]	56.3±9.8 [53.8,58.8]	20.9±7.7 [19.1,22.7]	16.0±3.5 [15.1,16.9]	0.004±0.01 [0.002,0.007]	0.03±0.05 [0.019,0.042]

Table 6 (Continued)

	Bandwidth knee(Hz) (CI)	Bandwidth Ankle(Hz) (CI)	MNF knee(Hz) (CI)	MNF Ankle(Hz) (CI)	Total PSD Knee(mv) (CI)	Total PSD Ankle(mv) (CI)
3rd Trimester	44.5±20.2 [39.9,49.1]	60.0±9.2 [57.7,62.2]	25.5±9.6 [23.0,28.0]	17.8±4.6 [16.8,18.9]	0.003±0.006 [0.001,0.004]	0.02±0.05 [0.012,0.034]
Term	51.0±17.6 [45.9,56.1]	59.5±11.9 [55.7,63.2]	23.2±14.4 [18.9,27.5]	16.6±3.8 [15.4,17.]	0.007±0.01 [0.004,0.009]	0.02±0.03 [0.012,0.031]
Postpartum	62.5±24.5 [57.4,67.5]	63.9±10.2 [61.8,66.3]	17.8±6.4 [16.5,19.2]	16.4±4.3 [15.5,17.3]	0.007±0.01 [0.005,0.009]	0.04±0.09 [0.025,0.059]
p-value	2E-11[A]*	4E-8[A]*	6E-11[A]*	0.02[A*]	2E-6[A]*	0.2[A]

Note. MNF=Mean Frequency, [A]p-value obtained with one-way ANOVA test, values reported as mean±sd, *=significant difference, Hz=Hertz, †Denotes which group served as the baseline for comparison.

5.13 Time-Frequency Domain: Total Energy of DWT Coefficients

The total energy of DWT coefficient of level 1 is presented in Figure 23A&B for both knee and ankle. In the knee, for the first level of DWT coefficient, significant difference was seen between the term and post-partum versus the non-pregnant women. The total energy of the second and third level of DWT are shown in Figure 23C&D and Figure 23E&F, respectively. There is a significant difference seen in the post-partum group versus other groups in the knee for the second and third levels of DWT coefficients. No differences between groups were seen in the total energy of all levels of DWT coefficients for the ankle.

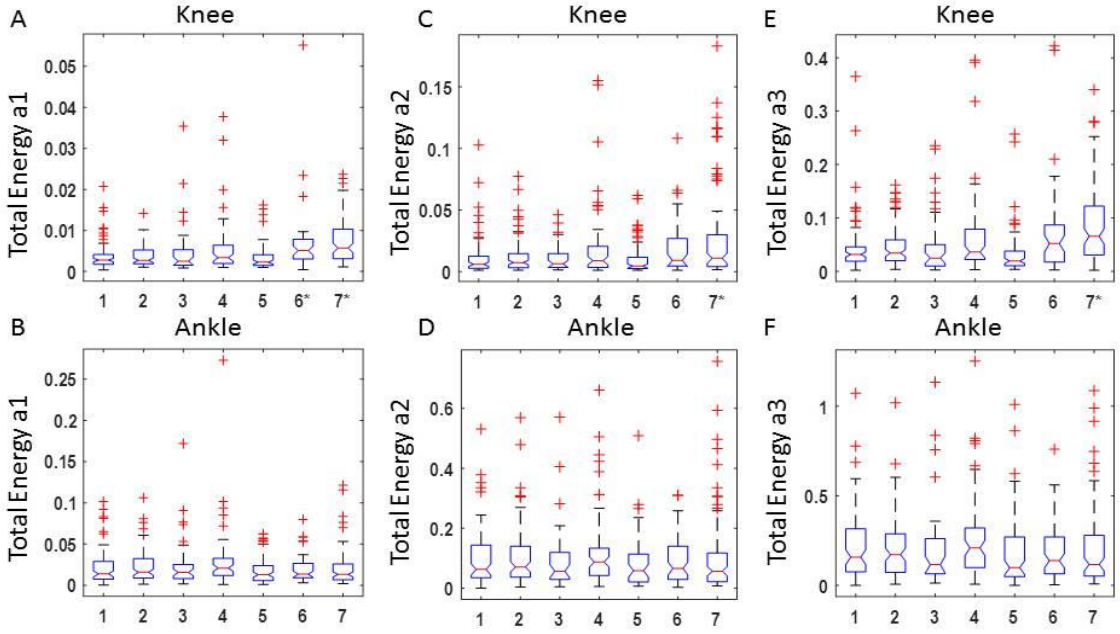

Figure 23. Total energy results of first three levels of the DWT coefficients are shown for all groups. Group designations are: 1- males, 2- non-pregnant females, 3- first trimester, 4-second trimester, 5-third trimester, 6-term and 7- post-partum.

5.14 Time-Frequency Domain: Total Energy of Intrinsic Mode Functions (IMFs)

The total energy of the first and second IMFs of EMD are shown in Figure 24for both knee and ankle. In the knee, significant difference is seen between both term and post-partum versus the non-pregnant women for the first IMF. For the second IMF significant difference was seen between the postpartum (as well as second trimester) versus other groups. No difference is seen between groups for the ankle reflex of the first and second IMFs.

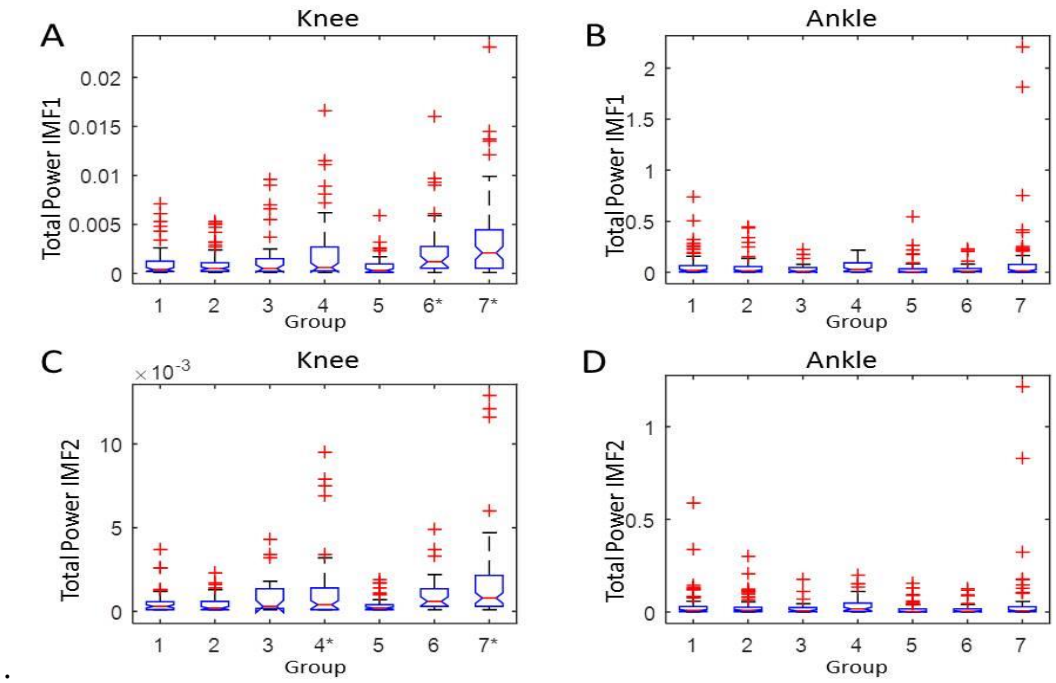

Figure 24. Total energy results of first and second IMFs of EMD are shown for all groups. Group designations are: 1- males, 2- non-pregnant females, 3-first trimester, 4-second trimester, 5-third trimester, 6-term and 7- post-partum. Time-Frequency Domain: Mean Frequency of IMFs

The mean frequencies of the first and second IMFs of EMD are presented in Figure 25for both knee and ankle. The MNF of the knee for the first and second IMFs decreased with the advancing the phase of pregnancy. In the knee, significant difference is seen earlier during the third trimester, as well as term and post-partum versus the non-pregnant women. For the second IMF, significant difference is seen later, between third trimester and postpartum and versus nonpregnant women. No difference between groups is seen in the MNF of the ankle reflex for the first and second IMFs.

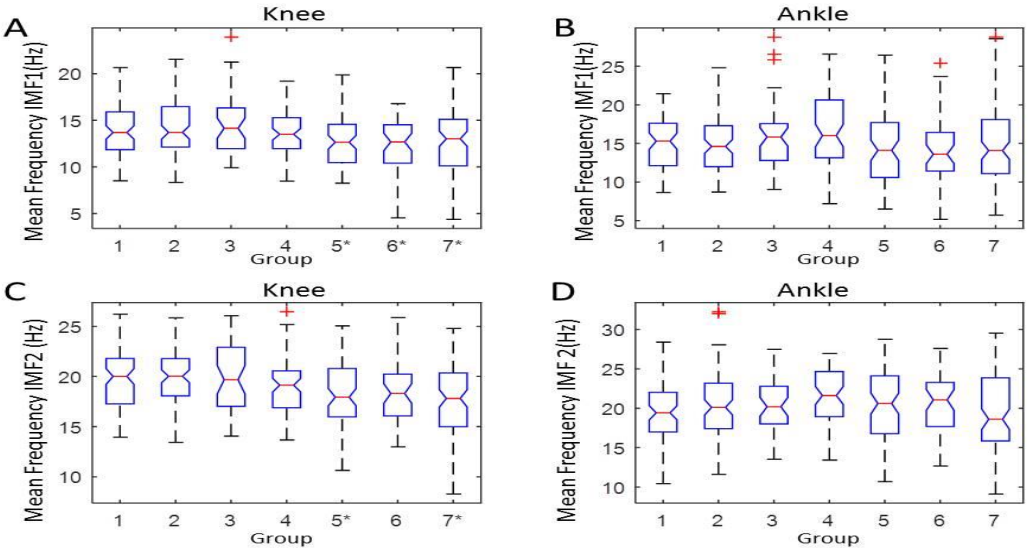

Figure 25. Mean frequency (MNF) results of first (A&B) and second IMFs (C&D) of EMD are shown all various groups. Group designations are: 1- males, 2- non-pregnant females, 3-first trimester, 4-second trimester, 5-third trimester, 6-term and 7- post-partum.

Table 7

Subjects' Time-Frequency Domain (DWT) Features and Their Confidence Intervals, By Group

	Total Energy a_1 Knee (CI)	Total Energy a_1 Ankle (CI)	Total Energy a_2 Knee (CI)	Total Energy a_2 Ankle (CI)	Total Energy a_3 Knee (CI)	Total Energy a_3 Ankle (CI)
Men	0.004±0.003 [0.003,0.004]	0.021±0.021 [0.016,0.025]	0.011±0.016 [0.008,0.014]	0.098±0.096 [0.078,0.012]	0.044±0.052 [0.032,0.055]	0.22±0.20 [0.177,0.264]
Non-pregnant	0.004± .003† [0.003,0.004]	0.023± 0.020 [0.019,0.027]	0.012± .014† [0.009,0.014]	0.10± 0.10 [0.081,0.12]	0.046± .037† [0.038,0.053]	0.21±0.18 [0.17,024]
1st Trimester	0.005±0.007 [0.003,0.007]	0.025±0.031 [0.015,0.035]	0.011±0.011 [0.007,0.014]	0.093±0.11 [0.06,0.13]	0.049±0.059 [0.031,0.067]	0.13±0.27 [0.049,0.059]
2nd Trimester	0.005±0.006 [0.004,0.007]	0.029±0.036 [0.020,0.038]	0.019±0.031 [0.012,0.027]	0.12±0.12 [0.094,0.16]	0.066±0.077 [0.047,0.084]	0.26±0.22 [0.20,0.31]
3nd Trimester	0.004±0.003 [0.003,0.004]	0.018±0.016 [0.014,0.022]	0.010±0.013 [0.007,0.013]	0.084±0.092 [0.057,0.11]	0.033±0.042 [0.023,0.042]	0.18±0.19 [0.13,0.22]
Term	0.007±0.009* [0.004,0.009]	0.020±0.017 [0.016,0.025]	0.019±0.023 [0.013,0.026]	0.093±0.082 [0.073,0.11]	0.072±0.087 [0.047,0.096]	0.18±0.16 [0.14,0.22]
Postpartum	0.007±0.005* [0.006,0.008]	0.020±0.021 [0.016,0.024]	0.025±0.035* [0.018,0.032]	0.11±0.13 [0.08,0.13]	0.086±0.070* [0.072,0.10]	0.20±0.22 [0.16,0.25]
P value	3E-07[A]*	0.1[A]	6E-05[A]*	0.5[A]	4E-08[A]*	0.3[A]

Note. [A]p-value obtained with one-way ANOVA test, values reported as mean±sd, *=significant difference, auHz= arbitrary unit•Hertz, †Denotes which group served as the baseline for comparison.

Table 8

Subjects' Time- Frequency Domain (Imfs) Features and Their Confidence Intervals, By Group

	Total Energy IMF 1 Knee (CI)	Total Energy IMF 1 Ankle (CI)	Total Energy IMF 2 Knee (CI)	Total Energy IMF 2 Ankle (CI)	MNF IMF1 knee (CI)	MNF IMF1 Ankle (CI)	MNF IMF2 knee (CI)	MNF IMF2 Ankle (CI)
Men	0.001±.001 [.00,0.001]	0.065±0.12 [.038,0.093]	0.001±.001 [0.00,0.001]	0.036±.082 [.017,0.055]	13.9±2.8 [13.3,14.4]	15.1±3.5 [14.2,15.9]	19.9±3.1 [19.25,20.6]	19.5±3.8 [18.6,20.4]
Non-pregnant	.001±.001† [0.00,0.001]	0.05±0.08 [.032,0.067]	.001±.001† [0.00,0.001]	0.027±.047 [.017,0.037]	14.3±2.9† [13.5,14.7]	14.9±3.6 [14.2,15.7]	19.9±2.7† [19.4,20.5]	20.1±4.0 [19.3,20.9]
1st Trimester	0.002±.003 [0.00,0.002]	0.032±.049 [.015,0.048]	0.001±.001 [0.00,0.001]	0.019±.034 [0.008,0.03]	13.4±3.2 [13.4,15.4]	18.8±4.4 [14.4,17.2]	19.9±3.1 [18.9,20.9]	20.5±3.6 [19.4,21.7]
2nd Trimester	0.002±.003 [.001,0.003]	0.05±0.06 [0.04,0.07]	.003±.004* [0.00,0.005]	0.033±.042 [.022,0.043]	13.5±2.4 [13.0,14.1]	16.4±4.5 [15.3,17.5]	19.2±2.8 [18.5,19.9]	21.6±3.9† [20.7,22.4]
3nd Trimester	0.001±.001 [0.00,0.001]	0.036±.079 [.018,0.055]	0.001±.002 [0.00,002]	0.015±.03 [.009,0.022]	12.6±2.6* [12.1,13.2]	14.5±4.4 [13.4,15.5]	18.2±3.2* [17.4,18.9]	20.5±4.2 [19.5,21.4]
Term	.002±.003* [.001,0.003]	0.034±.057 [.016,0.053]	0.001±.001 [0.001,002]	0.018±.031 [0.008,0.03]	12.3±2.7* [11.5,13.1]	14.1±4.5 [12.6,15.4]	18.4 ±2.9 [17.5,19.2]	20.9±3.9 [19.6,21.9]
Postpartum	.003±.004* [.002,0.004]	0.097±0.30 [0.036,016]	.002±.002* [.001,0.002]	0.046±0.15 [0.014,0.08]	12.8±3.5* [11.9, 13.4]	14.9±5.4 [13.8,16.0]	17.5±4.0* [16.7,18.4]	19.5±4.5* [18.6,20.5]
p-value	2e-90[A]*	0.12[A]	8e-7[A]*	0.25[A]	4e-05[A]*	0.09[A]	2e-07[A]*	0.03[A*]

Note. MNF=Mean Frequency, [A]p-value obtained with one-way ANOVA test, values reported as mean±sd, *=significant difference, auHz= arbitrary unit•Hertz, †Denotes which group served as the baseline for comparison.

Chapter 6

Discussion

Our work has demonstrated that DTRs can be quantitatively assessed, even in pregnancy. This is the second work to assess reflexes during pregnancy, and the first to assess both knee and ankle, the first to use frequency and time-frequency analysis and the first to find significant differences during pregnancy. The reflex response in its non-processed form, whether assessed subjectively or objectively, has significant variability from person to person and signal to signal. After signal processing and detailed study of the obtained DTR signal, our data showed that the most robust and measurable properties of lower extremity DTRs are latency in the time domain as well as bandwidth and mean frequency in frequency-domain. The amplitude has large variability making its analysis less meaningful. The duration does not show as many differences and as early as latency. Total energy is variable and contains many outliers, likely due to variability in being able to elicit a DTR. In this study, DTR was able to be elicited in 97% of patients. In this study we have quantitatively characterized knee and ankle reflexes in seven normotensive groups including men, non-pregnant women and five stages of pregnancy. We used the most pragmatic approach of manual strike with the most commonly used hammer. To date there are nine publications on normotensive electromyography data of the patellar reflex [14-16, 18, 20, 22-24, 27]. Kuruoglu and Oh [14], Frijns CJ *et al.* [15], Struys *et al.* [16] considered latency at two stations (knee and ankle). As far as we know Brussé *et al.*[22] were the first and only study that quantified the latency at the knee during pregnancy .The rest studies of DTR quantified latency in the knee of men and woman. The main findings of our study are as following:

There is a trend of increasing latency with increasing gestational age throughout pregnancy, which becomes significant in the term and post-partum period in the knee and post-partum in the ankle. Brussé *et al*. [22] has been published the first study of quantification deep tendon reflexes during pregnancy. They were not able to find any differences during any trimester of normotensive pregnancy. Several possible explanations of differences between our finding and their results are as following: 1) differentiation between measurement and quantification of the DTR signals. We investigated three different definitions of latency and found the best method to be peak to first peak, which had the smallest standard division as well as lowest number of outliers as opposed to the peak to onset definition which they used (we showed that peak to onset has the highest number of outliers). Jesunathadas *et al*.[40] have shown that due to the influence of amplitude cancellation (the overlap of opposing phase of different signals from individual motor unit action potential) determining the onset of the motor unit activity from surface EMG is not always accurate. Another reason for unreliability of onset detection may be artifact in the response signal from the hammer tap, which may delay the detection of response signal onset. 2) The number of tendon taps per patient in our study were 3 times higher than their study (30 versus 10) and we showed that 97% of subjects coverage to true value of the latency with 30 taps, when using the mode analysis introduced. Even when using the mode of latency (which was not used in that study) with 10 taps only 66% of data converge to true value of the latency; and likely fewer actually converged as they likely used mean analysis. 3) This study had a larger sample size of participations (279 versus 218). 4) They used the mean and we used the mode of trials and it has now been shown using the mode is more stable than the mean. The mean

method can contaminate the signals (due to outliers) and may led to erroneous interpretation of the signal due to impulse artifacts, signal variability and noise.

By considered both patellar and ankle reflexes during normotensive pregnancy, we have shown that the increase in the latency during pregnancy is constant and not a function of distance traveled. Therefore, we propose that the increase in the latency represents a central inhibition of the reflex arc at the level of the spinal cord (inhibitory brain effect at the synapse of the reflex arc in the anterior horn of the spinal cord) as opposed to a change in conduction velocity of the nerve (in which case one would expect the latency difference to double at the ankle compared to the knee due to the longer distance travelled). Therefore, the delay is felt to represent central inhibition of the reflex at the spinal cord rather than being explained by the potential perineural edema of pregnancy (central as opposed to peripheral nervous system effect). We further hypothesize that the gradual increase in latency throughout pregnancy is an inhibitory CNS effect gradually increasing over the course of pregnancy. To the authors' knowledge, we are not aware of any other studies to quantify deep tendon reflexes during pregnancy at two locations with surface EMG. This is one of the most novel and interesting findings of this work. Furthermore, the inhibitory effect of the brain on peripheral reflex arc may be a protective mechanism to prevent excitatory activity during pregnancy, which may be lost in patients who experience eclampsia. Therefore, by quantitation of the DTR and the normal ranges provided above, it may be possible to detect changes predisposing to eclampsia sooner and with higher sensitivity than currently used methods. Eogan *et al*.[55] showed in 2004 via upper extremity nerve conduction study that nerve conduction velocity slightly increases during pregnancy (they

showed an 11% reduction in latency in the ulnar nerve). This further shows that the increase in latency of DTR observed in this study is not due to a reduction in conduction velocity.

We found that the latency of the patellar reflexes profoundly dependent on the gender and the DTR is significantly faster in females compared with males. This finding agrees with other studies [27, 56]. Vickery *et al.* [27] showed that there is no correlation between the same sex latency and stature, but there is correlation between the combined sex and stature as we have corroborated in this study. Therefore, they concluded that the higher latency in males is due to a larger diameter in the vastus lateralis (VL) muscle fibers and innervating alpha-motor neurons of males compared to females and not due to taller height. Prior studies that found a correlation between latency and height, combined their data from different sexes and were therefore likely confounded [14, 16, 18, 20, 57, 58].

Several studies showed there is a linear increase in latency with age [14-16, 18, 57, 59, 60], thought to be due to slowing of nerve conduction velocity. All of these studies had large variations of subject ages: Kuruoglu and Oh [14] had age range of (16-58 years); Frijns *et al*. [15] had average age of (39.9$\pm$11.7 years); Pereon *et al*. [18] had age variation from 3 months infant to 80 years old; Gregersen G *et al*. [59] participants were aged (17-74 years); Rivner *et al*. [57] the variation of ages was (20-95 years); Chung SG *et al*. [60] compared latency in two ranges of age, young (ages=29.9$\pm$6.5 yrs) and elderly (ages=69.4$\pm$7 yrs). The variations of our participants' ages were smaller (ages = 25.9$\pm$6.9), and although the appropriate trend as to reduced conduction velocity

in the multiple linear regressions analysis was found, the range of ages was too small to require normalization.

In the frequency domain, bandwidth increased during pregnancy, mean frequency decreased and total energy increased, which are all new findings. Many of the frequency domain results seemed to corroborate the time domain analysis with significant differences found later in pregnancy. We found that the frequency-domain analysis, based on the bandwidth of the DTR response and the time-domain analysis, based on the peak-to-first peak latency, lead to the same results; namely, the postpartum group is significantly different from all other groups. Namely, the DTR latency and bandwidth were significantly prolonged in postpartum compared to normotensive non-pregnant in both knee and ankle. However, it must be noted that time domain and frequency domain are not reciprocal transforms when discussing surface EMG. Because, the latency of DTR probes nerve conduction, while the amplitude, duration of response signal and the spectral analysis probe the muscle contraction or motor units under the electrode (i.e. the effectors), albeit, we found an inverse relationship between the latency (delay) and mean frequency, which has been seen before in studies outside pregnancy. As far as we are aware, prior spectral (frequency domain) analyses were done in the surface EMG studies but not DTR studies. P. Phinyomark *et al*. have shown the usefulness of mean frequency in electromyography analysis for assessing muscle fatigue. Arendt-Nielsen *et al*. [61] showed a linear relationship between mean spectral frequencies (MNF) and conduction velocity in SEMG. In our study, while there was an increase in latency as well as a decrease in mean frequency, we do not believe in this case they are mediated by a reduced conduction velocity, since the latency changes in the knee and ankle are similar.

On the other hand, Dario Farina *et al.* [34] showed the spectral analysis of the surface EMG are intrinsic to the properties of the surface EMG signals such as depth of the MU, the placement of electrode and muscle size.

Basmajian, in 1970, established normal durations recordable by surface electrodes, of about 6-60 ms, or 14.50-150 Hz [62]. Since then, the frequency bandwidth of the EMG signal has been found to be concentrated between 15.6-250 Hz [62]. Our mean frequencies fall at the lower end of this range, possibly due to attenuation of higher frequencies when making a surface measurement. The reduction of mean frequency during pregnancy may relate to edema developing in the soft tissues.

We found that the variations of the amplitude are high which make them less useful. It has been argued that, since reflex amplitudes show a large inter- and intra-individual variability, they are less useful in characterizing the DTR signal [15, 20, 34, 44], which our results corroborate. Stam J *et al.* [9] and Dario Farina *et al.* [34] showed the thickness of the subcutaneous tissue, distribution of MU conduction velocities and the location of the electrode all effect and cause variation in signal amplitude. We found that the amplitude of the response signal in the ankle was at least 3 times bigger than the knee which is similar to Frijns CJ *et al.* results [15]. This may be due to the less fat in the calf compare to the thigh. Tham LK *et al.* [23] and Kim *et al.* [24] showed a linear relationship between the reflex amplitude and the hammer tapping angle. Their amplitude results were two times our amplitude at same tapping angle, which may be due to differences in subject characteristics or electrodes and system amplification. It can also be noted that our number of trials are 10 times that study (30 taps versus 3).

In this study, the DTR latency in the ankle were 1.8 times of the knee, which are very similar to the values (1.7) and (1.6) in Frijns *et al.* [15] and Kim *et al.* [24] studies, respectively, further demonstrating the accuracy of our latency measurements. The values of our latency in the knee and ankle are similar to Frijns *et al.* [15] as well as Vickery *et al.* [27]. Kuruoglu and Oh [14] found latency values in the knee that were 2.5 millisecond shorter than this study. This difference is likely due to different definitions of the latency (peak to first peak in this study) versus their study (the stimulus to the onset of the first deflection from the baseline) but could also be affected by different electrode placement or subject characteristics.

Chapter 7

Conclusions and Future Work

In conclusion, this study is the largest study to analyze deep tendon reflexes in pregnancy cohort to date. There have been significant knowledge generated regarding data acquisition, signal processing and biological implications.

In data acquisition, we performed the mean and mode analysis and found the convergence in mode is faster and more reliable compared to the mean. This allowed us to build stabilization curves as a function of the number of trials and we determined the optimal number of trials to minimize inter-subject variability.

In signal processing, we found that the definition of latency is important. We compared all definitions of latency with respect to within-subject variability as well as robustness to outliers and we found that the peak-to-first peak measure of latency is most robust in terms of minimum number of outliers and smallest standard deviation. We did a multi parametric fitting to remove the possible effect of age, weight and height, which showed there is no need to normalize the latency.

In biological implication, we found a trend of increasing latency with increasing gestational age throughout pregnancy, which becomes significant in the term at the knee and post-partum period at both stations. We established that the increase in the latency is caused by a central inhibition of the reflex arc at the level of the spinal cord rather than nerve conduction velocity. This result could only be asserted because we have measurements at both knee and ankle. The statistical significance of postpartum with non-pregnant group was reinforced by the frequency and time-frequency analysis. We found the bandwidth increases, MNF decreases and total energy increases in the knee

during pregnancy. We found the time-frequency domain analysis (EMD) allows earlier detection of changes in third trimester in the knee.

In future, we want to recruit subjects with pre-eclampsia and compare to normative data which are shown in the normality table and we want to produce user-friendly software for early diagnosis of eclampsia based on DTR signal characteristics.

References

[1] B. M. Sibai, "Diagnosis and management of gestational hypertension and preeclampsia," *Obstet Gynecol,* vol. 102, pp. 181-92, Jul 2003.

[2] A. K. Shah, K. Rajamani, and J. E. Whitty, "Eclampsia: a neurological perspective," *J Neurol Sci,* vol. 271, pp. 158-67, Aug 15 2008.

[3] A. G. Witlin, G. R. Saade, F. Mattar, and B. M. Sibai, "Risk factors for abruptio placentae and eclampsia: analysis of 445 consecutively managed women with severe preeclampsia and eclampsia," *Am J Obstet Gynecol,* vol. 180, pp. 1322-9, Jun 1999.

[4] B. M. Sibai, "Diagnosis, prevention, and management of eclampsia," *Obstet Gynecol,* vol. 105, pp. 402-10, Feb 2005.

[5] J. M. Alexander, D. D. McIntire, K. J. Leveno, and F. G. Cunningham, "Selective magnesium sulfate prophylaxis for the prevention of eclampsia in women with gestational hypertension," *Obstet Gynecol,* vol. 108, pp. 826-32, Oct 2006.

[6] B. M. Sibai, "Magnesium sulfate prophylaxis in preeclampsia: Lessons learned from recent trials," *Am J Obstet Gynecol,* vol. 190, pp. 1520-6, Jun 2004.

[7] L. S. Bickley and R. A. Hoekelman, *Bates' guide to phyisical examination and history taking*. Philadelphia: Lippincott Williams & Wilkins, 1999.

[8] S. Manschot, L. van Passel, E. Buskens, A. Algra, and J. van Gijn, "Mayo and NINDS scales for assessment of tendon reflexes: between observer agreement and implications for communication," *J Neurol Neurosurg Psychiatry,* vol. 64, pp. 253-5, Feb 1998.

[9] J. Stam and H. van Crevel, "Reliability of the clinical and electromyographic examination of tendon reflexes," *J Neurol,* vol. 237, pp. 427-31, Nov 1990.

[10] M. Hallett, "NINDS myotatic reflex scale," *Neurology,* vol. 43, p. 2723, Dec 1993.

[11] I. Litvan, C. A. Mangone, W. Werden, J. A. Bueri, C. J. Estol, D. O. Garcea, *et al.*, "Reliability of the NINDS Myotatic Reflex Scale," *Neurology,* vol. 47, pp. 969-72, Oct 1996.

[12] P. Dietrichson and R. Sorbye, "Clinical method for electrical and mechanical recording of the mechanically and electrically elicited ankel reflex," *Acta Neurol Scand,* vol. 47, pp. 1-21, 1971.

[13] J. Stam and J. R. Van Leeuwen, "A simple measurement hammer for quantitative reflex studies," *Electroencephalogr Clin Neurophysiol,* vol. 58, pp. 282-4, Sep 1984.

[14] R. Kuruoglu and S. J. Oh, "Quantitation of tendon reflexes in normal volunteers," *Electromyogr Clin Neurophysiol,* vol. 33, pp. 347-51, Sep 1993.

[15] C. J. Frijns, D. M. Laman, M. A. van Duijn, and H. van Duijn, "Normal values of patellar and ankle tendon reflex latencies," *Clin Neurol Neurosurg,* vol. 99, pp. 31-6, Feb 1997.

[16] M. A. Struys, E. J. Jonkman, and R. L. Strijers, "Measurement of patellar and ankle tendon reflexes in normal subjects," *Electromyogr Clin Neurophysiol,* vol. 37, pp. 13-8, Jan-Feb 1997.

[17] G. L. Marshall and J. W. Little, "Deep tendon reflexes: a study of quantitative methods," *J Spinal Cord Med,* vol. 25, pp. 94-9, Summer 2002.

[18] Y. Pereon, S. Nguyen The Tich, E. Fournier, R. Genet, and P. Guiheneuc, "Electrophysiological recording of deep tendon reflexes: normative data in children and in adults," *Neurophysiol Clin,* vol. 34, pp. 131-9, Oct 2004.

[19] R. Lemoyne, F. Dabiri, and R. Jafari, "Quantified deep tendon reflex device, second generation," *Journal of Mechanics in Medicine and Biology* vol. 8, pp. 75-85, 2008.

[20] J. Stam and H. van Crevel, "Measurement of tendon reflexes by surface electromyography in normal subjects," *J Neurol,* vol. 236, pp. 231-7, May 1989.

[21] M. Alisauskiene, M. R. Magistris, N. Vaiciene, and A. Truffert, "Electrophysiological evaluation of motor pathways to proximal lower limb muscles: a combined method and reference values," *Clin Neurophysiol,* vol. 118, pp. 513-24, Mar 2007.

[22] I. A. Brusse, G. H. Visser, I. C. van der Marel, S. Facey-Vermeiden, E. A. Steegers, and J. J. Duvekot, "Electromyographically recorded patellar reflex in normotensive pregnant women and patients with preeclampsia," *Acta Obstet Gynecol Scand,* vol. 94, pp. 376-82, Apr 2015.

[23] L. K. Tham, N. A. Abu Osman, W. A. Wan Abas, and K. S. Lim, "The validity and reliability of motion analysis in patellar tendon reflex assessment," *PLoS One,* vol. 8, p. e55702, 2013.

[24] Y. W. Kim, "Clinical availability of the deep tendon reflex test using a novel apparatus in healthy subjects," *J Phys Ther Sci,* vol. 27, pp. 317-20, Feb 2015.

[25] C. De Luca "The Use of Surface Electromyographyin Biomechanics " *JOURNAL OF APPLIED BIOMECHANICS,* vol. 13, pp. 135-163, 1977.

[26] K. R. Sharma, D. Saadia, A. G. Facca, S. Resnick, and D. R. Ayyar, "Diagnostic role of deep tendon reflex latency measurement in small-fiber neuropathy," *J Peripher Nerv Syst,* vol. 12, pp. 223-31, Sep 2007.

[27] H. S. Vickery and P. A. Smith, "Surface electromyography reveals males have a slower patellar reflex than females," *J Electromyogr Kinesiol,* vol. 22, pp. 990-6, Dec 2012.

[28] C. Y. Yang, X. Guo, Y. Ren, S. H. Kang, and L. Q. Zhang, "Position-dependent, hyperexcitable patellar reflex dynamics in chronic stroke," *Arch Phys Med Rehabil,* vol. 94, pp. 391-400, Feb 2013.

[29] P. W. Hodges and B. H. Bui, "A comparison of computer-based methods for the determination of onset of muscle contraction using electromyography," *Electroencephalogr Clin Neurophysiol,* vol. 101, pp. 511-9, Dec 1996.

[30] S. Solnik, P. Rider, K. Steinweg, P. DeVita, and T. Hortobagyi, "Teager-Kaiser energy operator signal conditioning improves EMG onset detection," *Eur J Appl Physiol,* vol. 110, pp. 489-98, Oct 2010.

[31] S. Solnik, P. DeVita, P. Rider, B. Long, and T. Hortobagyi, "Teager-Kaiser Operator improves the accuracy of EMG onset detection independent of signal-to-noise ratio," *Acta Bioeng Biomech,* vol. 10, pp. 65-8, 2008.

[32] A. Merlo, D. Farina, and R. Merletti, "A fast and reliable technique for muscle activity detection from surface EMG signals," *IEEE Trans Biomed Eng,* vol. 50, pp. 316-23, Mar 2003.

[33] D. A. Winter, *Kinematics, in Biomechanics and Motor Control of Human Movemen,* Fourth Edition ed. Hoboken, NJ, USA: John Wiley & Sons, Inc, 2009.

[34] D. Farina, R. Merletti, and R. M. Enoka, "The extraction of neural strategies from the surface EMG: an update," *J Appl Physiol (1985),* vol. 117, pp. 1215-30, Dec 1 2014.

[35] V. T. Inman, H. J. Ralston, J. B. Saunders, B. Feinstein, and E. W. Wright, Jr., "Relation of human electromyogram to muscular tension," *Electroencephalogr Clin Neurophysiol,* vol. 4, pp. 187-94, May 1952.

[36] J. V. Basmajian and D. , C.J., *Muscles Alive*. Baltimore, MD: Williams & Wilkins, 1985.

[37] N. Hogan and R. W. Mann, "Myoelectric signal processing: optimal estimation applied to electromyography--Part I: derivation of the optimal myoprocessor," *IEEE Trans Biomed Eng,* vol. 27, pp. 382-95, Jul 1980.

[38] E. Clancy and N. Hogan "EMG amplitude estimation from temporally whitened, spatially uncorrelated multiple channel EMG," *Ann Int Conf IEEE Eng Med Biol Soc,* vol. 12, p. 4, 1990.

[39] N. E. Huang and S. S. Shen, *Hilbert-Huang Transform and Its Applications*. NASA Goddard Space Flight Center, USA: World Scientific, 2005.

[40] M. Jesunathadas, S. S. Aidoor, K. G. Keenan, D. Farina, and R. M. Enoka, "Influence of amplitude cancellation on the accuracy of determining the onset of muscle activity from the surface electromyogram," *J Electromyogr Kinesiol,* vol. 22, pp. 494-500, Jun 2012.

[41] S. J. Day and M. Hulliger, "Experimental simulation of cat electromyogram: evidence for algebraic summation of motor-unit action-potential trains," *J Neurophysiol,* vol. 86, pp. 2144-58, Nov 2001.

[42] K. G. Keenan, D. Farina, K. S. Maluf, R. Merletti, and R. M. Enoka, "Influence of amplitude cancellation on the simulated surface electromyogram," *J Appl Physiol (1985),* vol. 98, pp. 120-31, Jan 2005.

[43] D. G. Simons and M. R. Dimitrijevic, "Quantitative variations in the force of quadriceps responses to serial patellar tendon taps in normal man," *Am J Phys Med,* vol. 51, pp. 240-63, Oct 1972.

[44] J. Stam and K. M. Tan, "Tendon reflex variability and method of stimulation," *Electroencephalogr Clin Neurophysiol,* vol. 67, pp. 463-7, Nov 1987.

[45] M. Hayes and *Statistical Digital Signal Processing and Modeling*. New York, NY, USA: John Wiley & Sons, Inc, 1996.

[46] D. Farina and R. Merletti, "Comparison of algorithms for estimation of EMG variables during voluntary isometric contractions," *J Electromyogr Kinesiol,* vol. 10, pp. 337-49, Oct 2000.

[47] S. Mallet, "A Theory for Multiresolution Signal Decomposition: The Wavelet Representation," *IEEE TRANSACTIONS ON PATTERN ANALYSIS AND MACHINE INTELLIGENCE,* vol. 2, 1989.

[48] M. Akay, "Wavelets in biomedical engineering," *Ann Biomed Eng,* vol. 23, pp. 531-42, Sep-Oct 1995.

[49] N. E. Huang, Z. Shen, S. R. Long, M. C. Wu, H. H. Shih, Q. Zheng, *et al.*, "The empirical mode decomposition and the Hilbert spectrum for nonlinear and non-stationary time series analysis " *Soc. Lond. A* vol. 454, pp. 903-995, 1998.

[50] A. Phinyomark, F. Quaine, S. Charbonnier, C. Serviere, F. Tarpin-Bernard, and Y. Laurillau, "Feature extraction of the first difference of EMG time series for EMG pattern recognition," *Comput Methods Programs Biomed,* vol. 117, pp. 247-56, Nov 2014.

[51] S. S. Ayache, T. Al-Ani, and J. P. Lefaucheur, "Distinction between essential and physiological tremor using Hilbert-Huang transform," *Neurophysiol Clin,* vol. 44, pp. 203-12, Apr 2014.

[52] D. Howell and S. M. f. P. D. p. I. 0-534-37770-X, *Statistical Methods for Psychology,* 2002.

[53] H. William, W. Kruskal , and W. Allen, "Use of Ranks in One-Criterion Variance Analysis," *Journal of the American Statistical Association,* vol. 47, 1952.

[54] S. E. Edgell and S. M. Noon, "Effect of violation of normality on the t test of the correlation coefficient," *Psychological Bulletin,* vol. 95, pp. 576-583, 1984.

[55] M. Eogan, C. O'Brien, D. Carolan, M. Fynes, and C. O'Herlihy, "Median and ulnar nerve conduction in pregnancy," *Int J Gynaecol Obstet,* vol. 87, pp. 233-6, Dec 2004.

[56] J. A. Morris, C. L. Jordan, and S. M. Breedlove, "Sexual differentiation of the vertebrate nervous system," *Nat Neurosci,* vol. 7, pp. 1034-9, Oct 2004.

[57] M. H. Rivner, T. R. Swift, and K. Malik, "Influence of age and height on nerve conduction," *Muscle Nerve,* vol. 24, pp. 1134-41, Sep 2001.

[58] H. Uysal, I. Mogyoros, and D. Burke, "Reproducibility of tendon jerk reflexes during a voluntary contraction," *Clin Neurophysiol,* vol. 110, pp. 1481-7, Aug 1999.

[59] G. Gregersen, "Diabetic neuropathy: influence of age, sex, metabolic control, and duration of diabetes on motor conduction velocity," *Neurology,* vol. 17, pp. 972-80, Oct 1967.

[60] S. G. Chung, E. M. Van Rey, Z. Bai, M. W. Rogers, E. J. Roth, and L. Q. Zhang, "Aging-related neuromuscular changes characterized by tendon reflex system properties," *Arch Phys Med Rehabil,* vol. 86, pp. 318-27, Feb 2005.

[61] L. Arendt-Nielsen and K. R. Mills, "Muscle fibre conduction velocity, mean power frequency, mean EMG voltage and force during submaximal fatiguing contractions of human quadriceps," *Eur J Appl Physiol Occup Physiol,* vol. 58, pp. 20-5, 1988.

[62] S. Karlsson and B. Gerdle, "Mean frequency and signal amplitude of the surface EMG of the quadriceps muscles increase with increasing torque--a study using the

continuous wavelet transform," *J Electromyogr Kinesiol,* vol. 11, pp. 131-40, Apr 2001.